Contribution from the Department of Chemistry,
The University of Michigan, Ann Arbor, Michigan 48109

# Octanuclear Heterometallic Clusters with Rhombic Dodecahedral Cores. The Synthesis, Structural Characterization, and Properties of the $\{Fe_6S_6(p\text{-}RPhO)_6[M(CO)_3]_2\}^{n-}$ Clusters (M = Mo, $n$ = 3, R = Me, OMe, $NMe_2$; M = W, $n$ = 3, R = Me; M = Mo, $n$ = 4, R = Me, OMe, COMe). Precursors for Synthetic Analogues for the Fe/Mo/S Site in Nitrogenase

S. A. Al-Ahmad, A. Salifoglou, M. G. Kanatzidis, W. R. Dunham, and D. Coucouvanis*

*Received May 22, 1989*

The synthesis and characterization of new members of the $[Fe_6S_6(p\text{-}RPhO)_6]^{3-}$ prismane series (R = OMe, $N(Me)_2$, COMe) and of the $\{Fe_6S_6(p\text{-}RPhO)_6[M(CO)_3]_2\}^{n-}$ adducts (M = Mo, $n$ = 3, R = Me, OMe, $NMe_2$; M = W, $n$ = 3, R = Me; M = Mo, $n$ = 4, R = Me, OMe, COMe) are described. The crystal and molecular structures of $(Et_4N)_3\{Fe_6S_6(p\text{-}OMePhO)_3\}$ (I), $(Et_4N)_3\{Fe_6S_6(p\text{-}OMePhO)_6[Mo(CO)_3]_2\}$ (II), $(Et_4N)_3\{Fe_6S_6(p\text{-}MePhO)_6[W(CO)_3]_2\}$ (III), and $(Et_4N)_4\{Fe_6S_6(p\text{-}COMePhO)_6[Mo(CO)_3]_2\}$ (IV) are described in detail. I crystallizes in the monoclinic space group $P2_1/n$ with cell dimensions $a$ = 14.699 (6) Å, $b$ = 12.008 (3) Å, $c$ = 44.026 (18) Å, $\beta$ = 91.77 (3)°, and $Z$ = 4. II crystallizes in the triclinic space group $P\bar{1}$ with cell dimensions $a$ = 12.581 (3) Å, $b$ = 13.0511 (2) Å, $c$ = 14.8404 (4) Å, $\alpha$ = 93.93 (2)°, $\beta$ = 89.96 (3)°, $\gamma$ = 116.087 (2)°, and $Z$ = 1. III crystallizes in the triclinic space group $P\bar{1}$ with cell dimensions $a$ = 12.352 (2) Å, $b$ = 13.402 (4) Å, $c$ = 14.375 (4) Å, $\alpha$ = 95.35 (2)°, $\beta$ = 93.81 (2)°, $\gamma$ = 63.27 (2)°, and $Z$ = 1. IV crystallizes in the triclinic space group $P\bar{1}$ with cell dimensions $a$ = 12.238 (4) Å, $b$ = 13.030 (5) Å, $c$ = 18.564 (9) Å, $\alpha$ = 92.80 (3)°, $\beta$ = 106.73 (4)°, $\gamma$ = 114.88 (3)°, and $Z$ = 1. Intensity data for I–IV were collected on a four-circle computer-controlled diffractometer with use of the $\theta$–$2\theta$ scan technique for II–IV and the $\omega$ scan technique for I. The structures were solved by conventional or direct-method techniques on 3410, 3253, 4336, and 3338 reflections for I–IV, respectively (for $I > 3\sigma(I)$). The structures were refined by full-matrix least-squares techniques (464 parameters for I, 468 parameters for II, 425 parameters for III, and 496 parameters for IV, to final $R$ values of 0.071 (I), 0.047 (II), 0.054 (III), and 0.054 (IV). Complex I contains the $(Fe_6S_6)^{3+}$ core, complexes II and III contain the $(Mo_2Fe_6S_6)^{3+}$ and $(W_2Fe_6S_6)^{3+}$ cores, respectively, and complex IV contains the $(Mo_2Fe_6S_6)^{2+}$ core. Coordination of the $M(CO)_3$ units to the $(Fe_6S_6)^{n+}$ central cages of II–IV results in an elongation of the latter along the idealized $\bar{6}$-fold axes. As a result of this elongation, the Fe–S bonds parallel to the $\bar{6}$-fold axes in II–IV are in the range from 2.338 (6) to 2.348 (4) Å and are significantly longer than the corresponding bonds in I at 2.309 (7) Å. The Mo–S distance in II at 2.614 (5) Å is slightly shorter than that in IV at 2.646 (8) Å, but similar to the W–S distance in III at 2.590 (3) Å. The Fe–M distances in II–IV are 2.99 (2), 2.96 (2), and 3.00 (2) Å. The electronic, cyclic voltammetric, and Mössbauer properties of the $\{Fe_6S_6(p\text{-}RPhO)_6\}^{n-}$ prismanes and the $\{Fe_6S_6(p\text{-}RPhO)_6[M(CO)_3]_2\}^{n-}$ adducts are affected by the type of para substituents and are discussed in detail. In the trianionic $Mo(CO)_3$ adducts, strongly electron-releasing para substituents on the terminal $p$-RPhO ligands, such as $-NMe_2$, facilitate the dissociation of one of the $Mo(CO)_3$ fragments and generation of the $\{Fe_6S_6(p\text{-}RPhO)_6[Mo(CO)_3]\}^{3-}$ heptametallic clusters.

## Introduction

Recent extensive studies on the Fe/Mo protein[1] component of nitrogenase and the nitrogenase cofactor[2] (FeMo(co)) have revealed in considerable detail the nature of a unique Fe/Mo/S aggregate intimately involved in biological $N_2$ fixation. In parallel with advances in understanding the nature of the Fe/Mo/S center in nitrogenase, a considerable interest in the basic coordination chemistry of Fe/Mo/S clusters has emerged with the goal of obtaining at least a structural analogue for this center. The stoichiometric and structural constraints imposed on the acceptability of synthetic analogues have been broadly defined from analytical and spectroscopic data on the Fe/Mo protein and the FeMo(co).

Originally the FeMo(co) was reported to contain iron, molybdenum, and sulfide in a 8:1:6 atomic ratio.[2] Subsequent analytical determinations gave Fe:Mo ratios of 7:1[3] and (8.2 ± 0.4):1.[4] The most recent analytical data on functional FeMo(co), isolated by a mild procedure, indicates[5] a Fe:Mo ratio of (5 ± 0.5):1. A similar fluctuation in analytical results also is apparent in several determinations of sulfur content and S:Mo ratios as low as 4:1[3] and as high as 9:1 or 8:1[4] have been reported.

Spectroscopic studies on the Fe/Mo protein by EPR and Mossbauer spectroscopy have shown six iron atoms each in a distinctive magnetic environment coupled to an overall $S = {}^3/_2$ spin system[6-8] and electron nuclear double resonance (ENDOR) studies suggest one molybdenum per spin system.[8] The $^{57}$Fe signals (five or six doublets) observed in the ENDOR spectra[8] possibly indicate an asymmetric structure for the Fe/Mo/S aggregate in which the iron atoms roughly can be grouped into two sets of trios, each set having very similar hyperfine parameters.

Extended X-ray absorption fine structure (EXAFS) studies on the Fe/Mo/S aggregate in nitrogenase have made available structural data that are essential in design of synthetic analogue clusters. Analyses of the Mo K-edge EXAFS of both the Fe/Mo protein and the FeMo(co)[9] have shown as major features three to four sulfur atoms in the first coordination sphere at 2.35 Å and two to three iron atoms further out from the Mo atom at ~2.7 Å. The Fe EXAFS of the FeMo(co)[10] shows the average iron

(1) Orme-Johnson, W. H. *Annu. Rev. Biophys. Biophys. Chem.* **1985**, *14*, 419–459.
(2) Shah, V. K.; Brill, W. J. *Proc. Natl. Acad. Sci. U.S.A.* **1977**, *74*, 3249.
(3) (a) Burgess, B. K.; Jacogs, D. B.; Stiefel, E. I. *Biochim. Biophys. Acta* **1980**, *614*, 196. (b) Newton, W. E.; Burgess, B. K.; Stiefel, E. I. In *Molybdenum Chemistry of Biological Significance*; Newton, W. E., Otsuka, S., Eds.; Plenum Press: New York, 1980; p 191. (c) Burgess, B. K.; Newton, W. E. In *Nitrogen Fixation*; Mueller, A., Newton, W. E., Eds.; Plenum Press: New York, 1983; p 83.
(4) Nelson, M. J.; Levy, M. A.; Orme-Johnson, W. H. *Proc. Natl. Acad. Sci. (U.S.A.)* **1983**, *80*, 147.
(5) Orme-Johnson, W. H.; Wink, D. A.; Mclean, P. A.; Harris, G. S.; True, A. E.; Hoffman, B.; Munck, E.; Papaefthymiou, V. *Recl. Trav. Chim. Pays-Bas* **1987**, *106*, 299.
(6) Rawlings, J.; Shah, V. K.; Chisnell, J. R.; Brill, W. J.; Zimmerman, R.; Munck, E.; Orme-Johnson, W. H. *J. Biol. Chem.* **1978**, *253*, 1001.
(7) Huynh, B. H.; Munck, E.; Orme-Johnson, W. H. *Biochim. Biophys. Acta* **1979**, *527*, 192.
(8) (a) Hoffman, B. M.; Roberts, J. E.; Orme-Johnson, W. H. *J. Am. Chem. Soc.* **1982**, *104*, 860. (b) Hoffman, B. M.; Venters, R. A.; Roberts, J. E.; Nelson, M.; Orme-Johnson, W. H. *J. Am. Chem. Soc.* **1982**, *104*, 4711.
(9) (a) Cramer, S. P.; Gillum, W. D.; Hodgson, K. O.; Mortenson, L. E.; Stiefel, E. I.; Chisnell, J. R.; Brill, W. J.; Shah, V. K. *J. Am. Chem. Soc.* **1978**, *100*, 4630. (b) Cramer, S. P.; Hodgson, K. O.; Gillum, W. O.; Mortenson, L. E. *J. Am. Chem. Soc.* **1978**, *100*, 3398.
(10) Antonio, M. R.; Teo, B. K.; Orme-Johnson, W. H.; Nelson, M. J.; Groh, S. E.; Lindahl, P. A.; Kauzlarich, S. M.; Averill, B. A. *J. Am. Chem. Soc.* **1982**, *104*, 4703.

0020-1669/90/1329-0927$02.50/0 

environment to consist of 3.4 ± 1.6 S(Cl) atoms at 2.25 (2) Å, 2.3 ± 0.9 Fe atoms at 2.66 (3) Å, 0.4 ± 0.1 Mo atoms at 2.76 (3) Å and 1.2 ± 1.0 O(N) atoms at 1.81 (7) Å. In the most recent Fe EXAFS study of the FeMo(co),[11] a second shell of Fe atoms was observed at a distance of 3.75 Å.

Collectively, the available structural and spectroscopic data on the Fe/Mo/S aggregate indicate an asymmetric arrangement of the Fe atoms relative to the Mo, in a cluster that may contain as structural features the $FeS_2Mo$ rhombic units. The Fe EXAFS data further suggest that about half of the iron atoms are at close proximity to the Mo atom (at 2.76 Å) and terminal ligation to the Fe atoms may involve O or N donor ligands.

Prior to 1978, only one Fe/Mo/S compound was known to contain the $FeS_2Mo$ structural unit. In this compound, $Cp_2Mo(S\text{-}n\text{-}Bu)_2FeCl_2$, the Mo and Fe atoms are bridged by two *n*-BuS$^-$ ligands.[12] Since then, numerous Fe/Mo/S complexes have been synthesized, and without exception they all contain $FeS_2Mo$ units. The majority of these complexes have been obtained by either the use of the $MoS_4^{2-}$ anion as a ligand in $MoS_4^{2-}/Fe(L)_n$ ligand-exchange reactions[13] or by spontaneous self assembly reactions that employ $MoS_4^{2-}$ as one of the reagents.[14,15] In general, oligonuclear Fe/Mo/S complexes are obtained by the former method and polynuclear clusters containing the $Fe_3MoS_4$ units are obtained by the latter method.

More recently, a synthetic approach that utilizes preformed Fe/S clusters and Mo reagents other than $MoS_4^{2-}$ has been used effectively in the synthesis of $[Fe_6S_6L_6(Mo(CO)_3)_2]^{n-}$[16] (from $[Fe_6S_6L_6]^{3-}$ and $(CH_3CN)_3Mo(CO)_3$), of $[MoOFe_5S_6(CO)_{12}]^{2-}$[17a] (from $[Fe_2S_2(CO)_6]^{2-}$ and $MoOCl_3\cdot 2THF$), and of $[MoOFe_6S_6(CO)_{16}]^{2-}$.[17b] With the exception of $[MoOFe_6S_6(CO)_{16}]^{2-}$, none of the Fe/Mo/S complexes isolated thus far shows a Fe:Mo ratio close to the approximate 6:1 ratio found in the nitrogenase cofactor. However, there exist Fe/Mo/S clusters that conceivably can serve as precursors for the synthesis of new clusters with a 6:1 Fe:Mo ratio and the simultaneous presence of acceptable structural features. One such class of clusters are the $\{Fe_6S_6L_6[Mo(CO)_3]_2\}^{n-}$ anions[16] ($n$ = 3, 4; L = Cl, ArO).

In this paper, we report in detail on the synthesis and characterization of the $[Fe_6S_6(p\text{-}RPhO)_6]^{n-}$ prismanes (R = MeO, $n$ = 3; R = $NMe_2$, $n$ = 3; R = COMe, $n$ = 3), the $\{Fe_6S_6(p\text{-}RPhO)_6[M(CO)_3]_2\}^{n-}$ adducts (M = Mo, R = MeO, $n$ = 3, 4; M = Mo, R = Me, $n$ = 3, 4; M = W, R = Me, $n$ = 3; M = Mo, R = $NMe_2$, $n$ = 3; M = Mo, AR = COMe, $n$ = 4) and the structural characterization of the $Et_4N^+$ salts of $[Fe_6S_6(p\text{-}MeOPhO)_6]^{3-}$ (I) and the $[Fe_6S_6(p\text{-}RPhO)_6(M(CO)_3)_2]^{n-}$ adducts (M = Mo, R = MeO, $n$ = 3 (II); M = W, R = Me, $n$ = 3 (III), M = Mo, R = COMe, $n$ = 4, (IV)).

## Experimental Section

**(1) Synthesis.** All procedures were carried out in an inert atmosphere by using a Vacuum Atmospheres Dri-Lab glovebox filled with prepurified nitrogen. The chemicals in this research other than solvents were used as purchased. Acetonitrile ($CH_3CN$) was distilled from calcium hydride ($CaH_2$) before use. *p*-(Dimethylamino)phenol was prepared as described in the literature.[18] Diethyl ether and methylene chloride ($CH_2Cl_2$) were distilled after being refluxed with $CaH_2$ for ~2 h. Sodium aryloxides were obtained by the reaction of sodium metal dispersion and the appropriate phenols in diethyl ether under nitrogen.

**(2) Physical Methods.** Visible and ultraviolet spectra were obtained on a Cary Model 219 spectrophotometer. Proton NMR spectra were obtained on a Bruker 300-MHz Pulse FT NMR spectrometer with $Me_4Si$ as internal standard. Chemical shifts are reported in parts per million (ppm). The following convention is used whenever isotropically shifted NMR spectra are reported. A positive sign is assigned to a resonance appearing downfield from $Me_4Si$. A negative sign is given to absorptions occurring upfield from $Me_4Si$.

Electrochemical measurements were performed with a PAR Model 173 potentiostat/galvanostat and a PAR Model 175 universal programmer. The electrochemical cell used had platinum working and auxiliary electrodes. As reference electrode, a saturated calomel electrode was used. All solvents used in the electrochemical measurements were properly dried and distilled, and tetra-*n*-butylammonium perchlorate ($Bu_4NClO_4$), was used as the supporting electrolyte. Normal concentrations used were ~0.001 M in electroanalyte and 0.1 M in supporting electrolyte. Purified argon was used to purge the solutions prior to the electrochemical measurements.

**Preparation of Compounds.** The procedure for the synthesis of one member of the $(Et_4N)_3[Fe_6S_6(ArO)_6]$, series (Ar = *p*-MePh) has been described elsewhere.[19] Pure crystalline compounds also are obtained in very good yields with Ar = *p*-EtPh and 2,4,6-$Me_3$Ph by using an identical procedure.

**Tris(tetraethylammonium) Hexakis(*p*-methoxyphenolato)hexakis-($\mu_3$-sulfido)hexaferrate(3II,3III), $(Et_4N)_3[Fe_6S_6(p\text{-}OMePhO)_6]$ (I).** To a solution of 1.0 g (0.85 mmol) of $(Et_4N)_3Fe_6S_6Cl_6$ in 30 mL of $CH_3CN$ was added 0.75 g, (5.14 mmol), of *p*-OMePhONa under continuous stirring. An immediate color change occurred upon mixing, from greenish brown to reddish brown. After 5 min of stirring, the reaction mixture was filtered to remove NaCl, and to the filtrate was added 120 mL of diethyl ether. When the mixture was allowed to stand overnight, a black microcrystalline solid was deposited. The product was collected by filtration, washed twice with diethyl ether, and dried under vacuum. The yield was 1.24 g (87.8%). Anal. Calcd for $Fe_6S_6O_{12}N_3C_{66}H_{102}$ (MW = 1657.2): Fe, 20.22; S, 11.60; N, 2.54; C, 47.83; H, 6.16. Found: Fe, 19.55; S, 11.02; N, 2.34; C, 46.66; H, 6.34.

**Tris(tetraethylammonium) Hexakis(*p*-(dimethylamino)phenolato)-hexakis($\mu_3$-sulfido)hexaferrate(3II,3III), $(Et_4N)_3\{Fe_6S_6[p\text{-}N(Me)_2PhO]_6\}$.** An amount of $(Et_4N)_3Fe_6S_6Cl_6$ (1.00 g, 0.85 mmol) and *p*-$N(Me)_2$PhONa (0.82 g, 5.16 mmol) were stirred in 30 mL of $CH_3CN$ for 5 min. The resulting reaction mixture was filtered to remove NaCl, and to the filtrate was added 120 mL of diethyl ether. When the mixture was allowed to stand overnight, a microcrystalline solid was deposited. The product was collected by filtration, washed twice with ether, and dried under vacuum. Yield: 1.25 g (84.5%). Anal. Calcd for $Fe_6S_6O_6N_9C_{72}H_{120}$ (MW 1735.5): Fe, 19.38; S, 11.07; N, 7.27; C, 49.83; H, 6.92. Found: Fe, 18.70; S, 10.48; N, 6.90; C, 48.15.

**Tris(tetraethylammonium) Hexakis(*p*-acetylphenolato)hexakis($\mu_3$-sulfido)hexaferrate(3II,3III), $(Et_4N)_3[Fe_6S_6(p\text{-}COMePhO)_6]$.** This compound was obtained in 84.8% yield by using a procedure identical with the one described above for the *p*-OMe derivative. No good (acceptable) analysis could be obtained for this cluster; however, the contact-shifted $^1H$ NMR spectrum in $CD_3CN$ solution (11.33 ppm (*m*-H), 1.28 ppm (*o*-H), and 3.4 ppm (*p*-COMe)) is characteristic for the $Fe_6S_6$ core.

**Tris(tetraethylammonium) Hexakis(*p*-methylphenolato)hexakis($\mu_4$-sulfido)hexaferrate(3II,3III)-Bis(tricarbonylmolybdenum(0)), $(Et_4N)_3\{Fe_6S_6(p\text{-}MePhO)_6[Mo(CO)_3]_2\}$.** To a 50 mL propionitrile solution of 0.80 g (0.51 mmol) of $[Et_4N]_3[Fe_6S_6(p\text{-}MePhO)_6]$ was added 0.54 g (1.78 mmol) of solid $(CH_3CN)_3Mo(CO)_3$.[20] The mixture was heated to ~90 °C for ca. 10 min. A color change to dark purple-red was observed, and the hot solution was filtered. After the solution was cooled to ambient temperature, 120 mL of diethyl ether was added to the filtrate, and when this mixture was allowed to stand for 4 h, a microcrystalline product formed and was isolated (0.85 g, 87% yield). This material is analytically pure; however, it can be recrystallized from $CH_3CH_2CN$ or $CH_3CN$ solutions upon the addition of diethyl ether and in the presence of $(CH_3CN)_3Mo(CO)_3$. Anal. Calcd for $Mo_2Fe_6S_6O_{12}N_3C_{72}H_{102}$ (MW 1920): Mo, 10.00; Fe, 17.5; S, 10.00; N, 2.18; H, 5.30;

(11) Arber, J. M.; Flood, A. C.; Garner, C. D.; Hasnain, S. S.; Smith, B. E. *J. Phys. Colloq.* **1986**, *47*, 1159.
(12) Cameron, T. S.; Prout, C. K. *Acta Crystallogr., Sect. B* **1972**, *B28*, 453.
(13) Coucouvanis, D. *Acc. Chem. Res.* **1981**, *14*, 201–209 and references therein.
(14) Holm, R. H.; Simhon, E. D. In *Molybdenum Enzymes*; Spiro, T. G., Ed.; Wiley-Interscience: New York, 1985; Chapter 1 and references therein.
(15) Christou, G.; Garner, C. D.; Mabbs, F. E.; King, T. J. *J. Chem. Soc., Chem. Commun.* **1978**, 740.
(16) (a) Coucouvanis, D.; Kanatzidis, M. G. *J. Am. Chem. Soc.* **1985**, *107*, 5005. (b) Kanatzidis, M. G.; Coucouvanis, D. *J. Am. Chem. Soc.* **1986**, *108*, 337. (c) Salifoglou, A.; Kanatzidis, M. G.; Coucouvanis, D. *J. Chem. Soc., Chem. Commun.* **1986**, 559. (d) Coucouvanis, D.; Salifoglou, A.; Kanatzidis, M. G.; Simopoulos, A.; Kostikas, A. *J. Am. Chem. Soc.* **1987**, *109*, 3807.
(17) (a) Bose, K. S.; Lamberty, P. E.; Kovacs, J. E.; Sin, E.; Averill, B. A. *Polyhedron* **1986**, *5*, 393–398. (b) Eldredge, P. A.; Bryan, R. F.; Sinn, E.; Averill, B. A. *J. Am. Chem. Soc.* **1988**, *10*, 5573.
(18) Weber, R.; Mueller, H. R. (Eprova AG). Gen. Offen. 2,649,229 (Cl. CO7C91/44), Nov 24, 1977; Swiss Appl. Nov. 14, 1975.
(19) Kanatzidis, M. G.; Salifoglou, A.; Coucouvanis, D. *Inorg. Chem.* **1986**, *25*, 2460.
(20) (a) Tate, D. P.; Knipple, W. R.; Augl, J. M. *Inorg. Chem.* **1962**, *1*, 433. (b) Ross, B. L.; Grasseli, J. G.; Ritchey, W. M.; Kaesz, H. D. *Inorg. Chem.* **1963**, *2*, 1023. (c) Stolz, I. W.; Dobson, G. R.; Sheline, R. K. *Inorg. Chem.* **1963**, *2*, 323.

C, 45.0. Found: Mo, 10.16; Fe, 18.03; S, 9.91; N, 2.29; H, 5.33; C, 44.82. X-ray powder pattern $d$ spacings (Å): 14.14 (vs), 12.03 (vs), 11.12 (vs), 9.21 (m), 7.45 (vw), 6.73 (vw), 6.26 (m), 5.45 (vw), 5.28 (vw), 4.55 (vw), 4.26 (w), 4.18 (w), 3.92 (vw), 3.64 (vw), 3.47 (vw), 3.25 (w), 3.02 (vw), 2.95 (vw), 2.78 (vw), 2.68 (vw), 2.61 (vw), 2.54 (vw), 2.37 (vw), 2.33 (vw), 2.23 (vw), 2.20 (vw), 2.14 (vw), 2.04 (vw), 1.95 (vw).

**Tris(tetraethylammonium) Hexakis($p$-methoxyphenolato)hexakis($\mu_4$-sulfido)hexaferrate(3II,3III)-Bis(tricarbonylmolybdenum(0)), $(Et_4N)_3\{Fe_6S_6(p\text{-}OMePhO)_6[Mo(CO)_3]_2\}$ (II). (i) From $(Et_4N)_3[Fe_6S_6(p\text{-}OMePhO)_6]$.** To a solution of 1.2 g (0.72 mmol) $(Et_4N)_3Fe_6S_6(p\text{-}OMePhO)_6$ in 30 mL of $CH_3CN$ was added 0.66 g (2.18 mmol) of $(CH_3CN)_3Mo(CO)_3$ with continuous stirring. The resulting reaction mixture was heated at 60 °C for 20 min. During that time, the color changed from brown-red to purple. The solution was filtered while hot and allowed to cool to room temperature. Subsequently, 120 mL of diethyl ether was added. When this mixture was allowed to stand for several hours, a black crystalline solid formed. The crystals were collected by filtration, washed twice with ether, and dried under vacuum. Yield: 1.3 g (88%). Anal. Calcd for $Mo_2Fe_6S_6O_{18}N_3N_3C_{72}H_{102}$ (MW = 2017): Mo, 9.92; Fe, 16.67; S, 9.52; N, 2.08; C, 42.86; H, 5.06. Found: Mo, 9.51; Fe, 17.05; S, 9.54; N, 1.96; C, 42.50; H, 4.84.

**(ii) From $(Et_4N)_2Fe_4S_4(p\text{-}OMePhO)_4$.** To a solution of $(Et_4N)_2[Fe_4S_4(p\text{-}OMePhO)_4]$ (1.0 g, 0.91 mmol) in 30 mL of $CH_3CN$ was added 0.42 g (1.39 mmol) of $(CH_3CN)_3Mo(CO)_3$ with continuous stirring. The resulting reaction mixture was heated at 60 °C for 20 min. The solution was then allowed to cool down to room temperature. Subsequently, it was filtered, and to the filtrate was added 100 mL of diethyl ether. When the mixture was allowed to stand for several hours, a crystalline solid formed. It was collected by filtration, washed with ether, and dried under vacuum. Yield: 0.95 g (80%) based on the amount of Fe. The UV/vis spectrum of the product in $CH_3CN$, the $^1H$ NMR spectrum, and the infrared spectrum all confirmed the identity of the product as $(Et_4N)_3\{Fe_6S_6(p\text{-}OMePhO)_6[Mo(CO)_3]_2\}$.

**(iii) From $(Et_4N)_2[Fe_2S_2(p\text{-}OMePhO)_4]$.** To a solution of 1.00 g, (1.08 mmol), of $(Et_4N)_2[Fe_2S_2(p\text{-}OMePhO)_4]$ in 30 mL of $CH_3CN$ was added 1.00 g (3.30 mmol) of $(CH_3CN)_3Mo(CO)_3$ under continuous stirring. The resulting solution was heated at 60 °C for 20 min. During that time, the color of the reaction mixture changed from brownish purple to purple. The solution was then allowed to cool to room temperature. Subsequently, it was filtered, and to the filtrate was added 120 mL of diethyl ether. When the mixture was allowed to stand for several hours, a crystalline solid formed. It was collected by filtration, washed twice with ether, and dried under vacuum. The yield was 0.40 g (60%), based on the amount of Fe. The UV/vis spectrum in $CH_3CN$, the $^1H$ NMR spectrum and the infrared spectrum confirmed the identity of the product as $(Et_4N)_3\{Fe_6S_6(p\text{-}OMePhO)_6[Mo(CO)_3]_2\}$.

**Tris(tetraethylammonium) Hexakis($p$-(dimethylamino)phenolato)hexakis($\mu_4$-sulfido)hexaferrate(3II,3III)-Bis(tricarbonylmolybdenum(0)), $(Et_4N)_3\{Fe_6S_6(p\text{-}NMe_2PhO)_6[Mo(CO)_3]_2\}$.** To a solution of 1.0 g of $(Et_4N)_3[Fe_6S_6(p\text{-}NMe_2PhO)_6]$, (0.58 mmol), in 30 mL of acetonitrile was added 0.53 g (1.75 mmol) of $(CH_3CN)_3Mo(CO)_3$ under continuous stirring. After the mixture was stirred for 30 min at room temperature, the color became purple-blue. The resulting solution was filtered, and to the filtrate was added 120 mL of diethyl ether. When this mixture was allowed to stand for 12 h, a black crystalline solid formed. The solid was collected, washed with ether several times, and dried under vacuum. Yield: 1.0 g (80%). Anal. Calcd for $Mo_2Fe_6S_6O_{12}N_9C_{78}H_{120}$ (MW = 2095): Mo, 9.17; Fe, 16.04; S, 9.17; N, 6.02; C, 44.70; H, 5.73. Found: Mo, 9.76; Fe, 16.9; S, 9.19; N, 5.67; C, 44.88; H, 5.50.

**Tris(tetraethylammonium) Hexakis($p$-methylphenolato)hexakis($\mu_4$-sulfido)hexaferrate(3II,3III)-Bis(tricarbonyltungsten(0)), $(Et_4N)_3\{Fe_6S_6(p\text{-}MePhO)_6[W(CO)_3]_2\}$ (III).** To a 40 mL $CH_3CN$ solution of 0.60 g (0.38 mmol) of $(Et_4N)_3[Fe_6S_6(p\text{-}MePhO)_6]$ was added, slowly with stirring, a warm solution of 0.60 g, (1.53 mmol), of $(CH_3CN)_3W(CO)_3$[19] in 30 mL of $CH_3CN$. The reaction mixture was heated to ~80 for 30–35 min, and the color changed to a dark purple red. The solution was allowed to cool to ambient temperature and then filtered. To the filtrate was added ~5 mL of tetrahydrofuran and 12 mL of diethyl ether were added. When this mixture was allowed to stand for 48 h, a microcrystalline product formed and was isolated (0.50 g, 62% yield). The compound was found to be X-ray isomorphous to the Mo analogue. Anal. Calcd for $W_2Fe_6S_6O_{12}N_3C_{72}H_{102}$ (MW = 2096): W, 17.56; Fe, 16.03; S, 9.16; N, 2.00; H, 4.87; C, 41.22. Found: W, 17.61; Fe, 17.09; S, 9.46; N, 2.35; H, 5.26; C, 41.12.

**Tetrakis(tetraethylammonium) Hexakis($p$-acetylphenolato)hexakis($\mu_4$-sulfido)hexaferrate(4II,2III)-Bis(tricarbonylmolybdenum(0)), $(Et_4N)_4\{Fe_6S_6(p\text{-}COMePhO)_6[Mo(CO)_3]_2\}$ (IV).** A solution of $(Et_4N)_3[Fe_6S_6(p\text{-}COMePhO)_6]$ (1.13 mmol) was prepared in situ by the reaction of $(Et_4N)_3(Fe_6S_6Cl_6)$ (1.3 g, 1.13 mmol) with $p$-COMePhONa (1.1 g, 7.0 mmol) in 30 mL of $CH_3CN$. To this solution, after filtration to remove the NaCl byproduct, was added solid $(CH_3CN)_3Mo(CO)_3$ (1.1 g, 3.4 mmol). After the mixture was heated to ca. 60 °C for ~40 min the resulting greenish brown solution was filtered and allowed to cool to ambient temperature. Upon addition of diethyl ether (30 mL), with the mixture kept standing for 1 h, a black powder appeared in suspension. This powder was isolated by filtration, and the filtrate was allowed to stand overnight at ambient temperature. The black crystals that formed were isolated, washed with ether, and dried (0.9 g). An additional 0.2 g of crystalline product was obtained upon recrystallization ($CH_3CN$/ether) of the initially isolated black powder. The overall yield was 1.1 g (57%), based on the $(Et_4N)_3(Fe_6S_6Cl_6)$ used. Anal. Calcd for $Mo_2Fe_6S_6O_{18}N_4C_{86}H_{122}$ (MW = 2219): Mo, 8.66; Fe, 15.15; S, 8.66; N, 2.52; C, 46.53; H, 5.50. Found: Mo, 8.68; Fe, 15.0; S, 8.65; N, 2.75; C, 46.65; H, 5.55. The same compound, $(Et_4N)_4\{Fe_6S_6(p\text{-}COMePhO)_6[Mo(CO)_3]_2\}$, can be obtained in 50% yields by using either $(Et_4N)_2[Fe_4S_4(p\text{-}COMePhO)_4]$ or $(Et_4N)_2[Fe_2S_2(p\text{-}COMePhO)_4]$ in otherwise identical synthetic procedures.

**Tetrakis(tetraethylammonium) Hexakis($p$-methoxyphenolato)hexakis($\mu_4$-sulfido)hexaferrate(4II,2III)-Bis(tricarbonylmolybdenum(0)), $(Et_4N)_4\{Fe_6S_6(p\text{-}OMePhO)_6[Mo(CO)_3]_2\}$.** To a solution of 1.0 g (0.5 mmol) of $(Et_4N)_3\{Fe_6S_6(p\text{-}OMePhO)_6[Mo(CO)_3]_2\}$ in 30 mL of acetonitrile was added a solution of 0.22 g (1.52 mmol) of $(Et_4N)BH_4$ in 5 mL acetonitrile under continuous stirring. After the mixture was stirred for 30 min, the color changed from purple to brown. The solution was then filtered, and to the filtrate was added 120 mL of diethyl ether. When this mixture was allowed to stand for several hours, a black microcrystalline solid formed. The product was collected by filtration, washed twice with ether, and dried under vacuum. Yield: 0.85 g (79.9%). Anal. Calcd for $Mo_2Fe_6S_6O_{18}N_4C_{80}H_{122}$ (MW = 2147): Mo, 8.93; Fe, 15.61; S, 8.96; N, 2.61; C, 44.74; H, 5.74. Found: Mo, 8.3; Fe, 16.1; S, 8.5; N, 2.7; C, 44.1; H, 5.5.

**Tetrakis(tetraethylammonium) Hexakis($p$-methylphenolato)hexakis($\mu_4$-sulfido)hexaferrate(4II,2III)-Bis(tricarbonylmolybdenum(0)), $(Et_4N)_4\{Fe_6S_6(p\text{-}MePhO)_6[Mo(CO)_3]_2\}$.** To a solution of 1.0 g (0.52 mmol) of $(Et_4N)_3\{Fe_6S_6(p\text{-}MePhO)_6[Mo(CO)_3]_2\}$ was added a solution of 0.22 g (1.86 mmol) of $(Et_4N)BH_4$ in 5 mL of acetonitrile. After the mixture was stirred for 30 min, the color changed from purple to brown. The resulting reaction mixture was then filtered, and to the filtrate was added 100 mL of diethyl ether. When this mixture was allowed to stand for 10 h, a black microcrystalline solid formed. The product was collected by filtration, washed twice with diethyl ether, and dried under vacuum. Yield: 0.98 g (91.8%). Anal. Calcd for $Mo_2S_6O_{12}N_4C_{80}H_{122}$ (MW = 2050): Mo, 9.37; Fe, 16.39; S, 9.37; N, 2.73; C, 46.83; H, 5.95. Found: Mo, 8.98; Fe, 15.9; S, 10.33; N, 2.73; C, 46.3; H, 5.73.

## X-ray Diffraction Measurements

**(a) Collection of Data.** Single crystals of $(Et_4N)_3[Fe_6S_6(p\text{-}OMePhO)_3]$ (I), $(Et_4N)_3[Fe_6S_6(p\text{-}OMePhO)_6[Mo(CO)_3]_2]$ (II), $(Et_4N)_3\{Fe_6S_6(p\text{-}MePhO)_6[W(CO)_3]_2\}$ (III), and $(Et_4N)_4\{Fe_6S_6(p\text{-}COMePhO)_6[Mo(CO)_3]_2\}$ (IV) were obtained by the slow diffusion of diethyl ether into acetonitrile solutions of the complexes. A single crystal of each complex was mounted in a thin-walled capillary under nitrogen and sealed to protect from air and moisture. The X-ray crystallographic data for I, II, and IV were obtained on a Nicolet P3/F four-circle computer-controlled diffractometer. The data for III were collected on a Syntex $P2_1$ four-circle computer-controlled diffractometer. A detailed description of the instrument and the data acquisition procedures have been given previously.[21] Intensity data were obtained by using graphite-monochromatized Mo K$\alpha$ radiation over one-fourth of the reciprocal lattice sphere for I and half of the reciprocal lattice sphere for II–IV. Because of the rapid decomposition of the crystal of III in the X-ray beam, at ambient temperature, the intensity data were collected at −84 °C by passing a stream of evaporating nitrogen over the crystal.

For each of the four structures, the unit cell was determined from 12 well-centered reflections whose $x$ and $y$ coordinates were obtained from random orientation photographs. Accurate cell parameters were obtained from a least-squares fit of the angular settings ($2\theta$, $\omega$, $\phi$, $\chi$) of 25 machine-centered reflections with $2\theta$ values between 20° and 40°. Details concerning crystal characteristics and X-ray diffraction methodology are shown in Table I.

**(b) Reduction of Data.** The raw data were reduced to net intensities, estimated standard deviations were calculated on the basis of counting statistics, Lorentz–polarization corrections were applied, and equivalent reflections were averaged. The estimated standard deviation of the structure factor was taken as the larger of that derived from counting statistics and that derived from the scatter of multiple measurements.

The least-squares program used minimizes $\sum w(|\Delta F|)^2$. The weighting function used throughout the refinement of the structure gives zero

(21) Kanatzidis, M. G.; Coucouvanis, D. *Inorg. Chem.* **1984**, *23*, 4192.

**Table I.** Summary of Crystal Data, Intensity Collection, and Structure Refinement of $(Et_4N)_3[Fe_6S_6(p\text{-}OMePhO)_6]$ (I), $(Et_4N)_3\{Fe_6S_6(p\text{-}OMePhO)_6[Mo(CO)_3]_2\}$ (II), $(Et_4N)_3\{Fe_6S_6(p\text{-}MePhO)_6[W(CO)_3]_2\}$ (III), and $(Et_4N)_4\{Fe_6S_6(p\text{-}COMePhO)_6[Mo(CO)_3]_2\}$ (IV)

| | I | II | III | IV |
|---|---|---|---|---|
| formula | $Fe_6S_6O_{12}N_3C_{66}H_{102}$ | $Mo_2Fe_6S_6N_3O_{18}C_{72}H_{102}$ | $W_2Fe_6S_6N_3O_{12}C_{72}H_{102}$ | $Mo_2Fe_6S_6N_4O_{18}C_{80}H_{122}$ |
| MW | 1657 | 2017 | 2096 | 2219 |
| $a$, Å | 14.699 (6) | 12.581 (3) | 12.352 (2) | 12.238 (4) |
| $b$, Å | 12.008 (3) | 13.0511 (2) | 13.402 (4) | 13.030 (5) |
| $c$, Å | 44.03 (2) | 14.8404 (4) | 14.375 (4) | 18.564 (9) |
| $\alpha$, deg | 90.00 | 93.93 (2) | 95.35 (2) | 92.80 (3) |
| $\beta$, deg | 91.77 (3) | 89.96 (2) | 93.81 (2) | 106.73 (4) |
| $\gamma$, deg | 90.00 | 116.087 (2) | 63.27 (2) | 114.88 (3) |
| $V$, Å$^3$; $Z$ | 7767 (5); 4 | 2182 (1); 1 | 2115 (1); 1 | 2522 (2); 1 |
| $d_{calcd}$, g/cm$^3$ | 1.43 | 1.53 | 1.65 | 1.46 |
| $d_{obsd}$, g/cm$^3$ | 1.41[a] | 1.51[a] | 1.60[b] | 1.43[a] |
| space group | $P2_1/n$ | $P\bar{1}$ | $P\bar{1}$ | $P\bar{1}$ |
| cryst dimens, mm | 0.29 × 0.55 × 0.05 | 0.09 × 0.26 × 0.62 | 0.28 × 0.13 × 0.56 | 0.15 × 0.42 × 0.08 |
| $\mu$, cm$^{-1}$ | 13.3 | 14.4 | 39.3 | 12.2 |
| radiation | Mo K$\alpha$[c] | Mo K$\alpha$[c] | Mo K$\alpha$[c] | Mo K$\alpha$[c] |
| data collecd | $2\theta$ = 0–45° | $2\theta$ = 0–40° | $2\theta$ = 0–45° | $2\theta$ = 0–45° |
| no. of data used ($F_o^2 > 3\sigma(F_o^2)$) | 3410 | 3253 | 4336 | 3338 |
| no. of params | 464 | 468 | 425 | 496 |
| $R$[d] | 0.071 | 0.047 | 0.054 | 0.054 |
| $R_w$[d] | 0.071 | 0.047 | 0.056 | 0.054 |

[a] Obtained by flotation in a $CCl_4$/hexane mixture. [b] Obtained by flotation in a $CHBr_3$/pentane mixture. [c] $\lambda$ = 0.710 69 Å. [d] $R = \sum||F_o| - |F_c||/|F_o|$. [e] $R_w = [\sum w(|F_o| - |F_c|)^2/\sum w|F_o|^2]^{1/2}$.

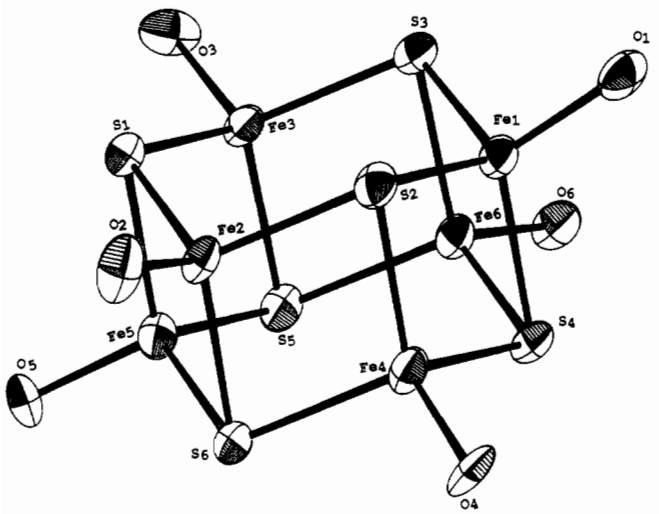


**Figure 1.** Structure and labeling of the $[Fe_6S_6(p\text{-}OMePhO)_6]^{3-}$ anion in I. The $p$-OMePh rings have been omitted for clarity. Thermal ellipsoids as drawn by ORTEP represent the 50% probability surfaces.

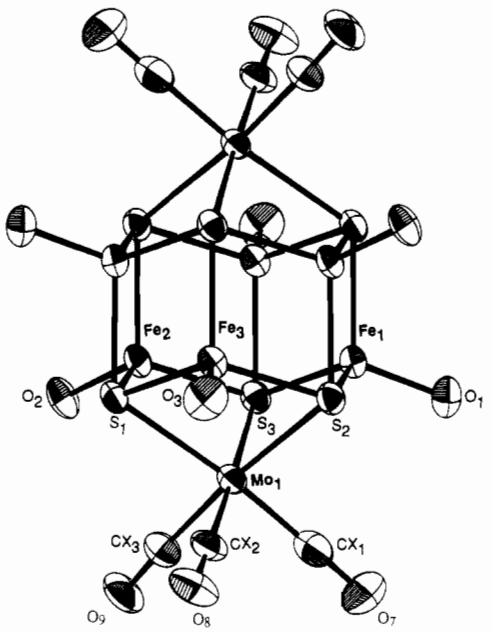


**Figure 2.** Structure and labeling of the anions in the $\{Fe_6S_6(p\text{-}RPhO)_6[M(CO)_3]_2\}^{n-}$ clusters in II (M = Mo, $n$ = 3, R = OMe), in III (M = W, $n$ = 3, R = Me), and in IV (M = Mo, $n$ = 4, R = COMe). The $p$-RPh rings have been omitted for clarity. Thermal ellipsoids as drawn by ORTEP represent the 50% probability surfaces.

weight to those reflections with $F^2 < 3\sigma(F^2)$ and $w = 1/\sigma^2(F)$ to all others,[22] where $\sigma^2(F) = \sigma_1^2(F) + [\text{abs}(g)]F^2$ ($g$ = 0.0002). No corrections for secondary extinction were applied to the data sets for I–IV. The atomic scattering factors of the neutral atoms were used, and all the scattering factors[23] except those for hydrogen were corrected by adding real and imaginary terms to account for the effects of anomalous dispersion.[24] The spherical hydrogen scattering factor tables of Stewart et al.[25] were used.

Due to the small $\mu$ values (Table I) and the small size of the crystals, no absorption corrections were applied. The refinement calculations were carried out on the University of Michigan Amdahl 800 computer by using the locally adapted SHELX76 crystallographic program package.[26]

**(c) Determination of Structures.** The structures of I–IV were determined by using data sets to $2\theta$ maxima of 40°. Three dimensional Patterson synthesis maps along with the direct-methods routine SOLV of the SHELXTL 84 package of crystallographic programs were employed to locate Fe, Mo, or W atoms. Subsequent difference Fourier maps were used to locate the sulfur atoms and the other non-hydrogen atoms in the asymmetric units. With four molecules in the unit cell of I the $[Fe_6S_6(p\text{-}OMePhO)_6]^{3-}$ anion and all three of the $Et_4N^+$ counterions in the asymmetric unit are situated on general positions. The unit cells of II–IV are triclinic (space group $P\bar{1}$), and each contains one formula unit per unit cell (Table I). As a result, in the structures of II–IV, the anions $\{Fe_6S_6(p\text{-}OMePhO)_6[Mo(CO)_3]_2\}^{3-}$, $\{Fe_6S_6(p\text{-}MePhO)_6[W(CO)_3]_2\}^{3-}$, and $\{Fe_6S_6(p\text{-}COMePhO)_6[Mo(CO)_3]_2\}^{4-}$ are required by symmetry to reside on crystallographic inversion centers. The two tetraethylammonium cations in the asymmetric unit of IV are located on general positions, and their structures are unexceptional. One of the cations in each of the structures of II and III is sitting on a general position and the other one is sitting on a center of symmetry (0, 0, 0.5). As a result the latter cations are subject to a 2-fold disorder.

**(d) Crystallographic Results.** The final atomic positional parameters for $(Et_4N)_3[Fe_6S_6(p\text{-}OMePhO)_6]$ (I), $(Et_4N)_3\{Fe_6S_6(p\text{-}OMePhO)_6[Mo(CO)_3]_2\}$ (II), $(Et_4N)_3\{Fe_6S_6(p\text{-}MePhO)_6[W(CO)_3]_2\}$ (III), and $(Et_4N)_4\{Fe_6S_6(p\text{-}COMePhO)_6[Mo(CO)_3]_2\}$ (IV) with standard deviations are shown in Tables II–V). Intermolecular distances and angles are given in Table VI. The numbering scheme for the anion in I is shown in Figure 1. That for the anions in II–IV is shown in Figure 2.

(22) Grant, D. F.; Killean, R. C. G.; Lawrence, J. L. *Acta Crystallogr., Sect. B* **1969**, *B25*, 374.
(23) Doyle, P. A.; Turner, P. S. *Acta Crystallogr., Sect. A* **1968**, *A24*, 390.
(24) Cromer, D. T.; Liberman, D. J. *J. Chem. Phys.* **1970**, *53*, 1891.
(25) Stewart, R. F.; Davidson, E. R.; Simpson, W. T. *J. Chem. Phys.* **1965**, *42*, 3175.
(26) *SHELXTL Package of Crystallographic Programs*; Nicolet XRD Corp.: Fremont, CA.

**Table II.** Fractional Atomic Coordinates[a] and Equivalent Isotropic Thermal Parameters for the Non-Hydrogen Atoms in $(Et_4N)_3[Fe_6S_6(p\text{-}OMePhO)_6]$ (I)

| atom | x | y | z | U, Å² | atom | x | y | z | U, Å² |
|---|---|---|---|---|---|---|---|---|---|
| Fe1 | 0.4061 (2) | 0.1114 (3) | 0.1553 (1) | 0.046 | C27 | 0.0929 (14) | 0.3487 (18) | 0.1756 (5) | 0.049 |
| Fe2 | 0.1667 (2) | 0.1090 (3) | 0.1166 (1) | 0.046 | O10 | −0.0290 (12) | 0.5996 (16) | 0.1979 (4) | 0.097 |
| Fe3 | 0.3354 (2) | −0.1272 (3) | 0.1029 (1) | 0.043 | C28 | −0.0261 (21) | 0.6707 (27) | 0.1716 (7) | 0.128 |
| Fe4 | 0.2267 (2) | 0.1195 (3) | 0.1764 (1) | 0.047 | C29 | 0.0046 (17) | −0.2156 (22) | 0.0910 (5) | 0.060 |
| Fe5 | 0.1614 (2) | −0.1228 (3) | 0.1242 (1) | 0.046 | C30 | −0.0178 (14) | −0.1114 (19) | 0.0768 (4) | 0.050 |
| Fe6 | 0.3975 (2) | −0.1156 (3) | 0.1636 (1) | 0.044 | C31 | −0.0843 (16) | −0.1120 (21) | 0.0526 (5) | 0.066 |
| S1 | 0.2171 (4) | −0.0220 (5) | 0.0841 (1) | 0.045 | C32 | −0.1272 (16) | −0.2043 (22) | 0.0429 (5) | 0.059 |
| S2 | 0.2864 (4) | 0.2118 (5) | 0.1358 (1) | 0.049 | C33 | −0.1079 (16) | −0.2986 (21) | 0.0553 (5) | 0.063 |
| S3 | 0.4523 (4) | −0.0234 (5) | 0.1220 (1) | 0.048 | C34 | −0.0389 (18) | −0.3121 (22) | 0.0790 (6) | 0.079 |
| S4 | 0.3465 (4) | 0.0193 (5) | 0.1962 (1) | 0.045 | O11 | −0.1955 (12) | −0.2101 (15) | 0.0200 (4) | 0.090 |
| S5 | 0.2816 (4) | −0.2241 (5) | 0.1439 (1) | 0.048 | C35 | −0.2174 (17) | −0.1071 (23) | 0.0078 (5) | 0.084 |
| S6 | 0.1098 (4) | 0.0088 (6) | 0.1567 (1) | 0.049 | C36 | 0.5499 (15) | −0.2666 (19) | 0.1694 (5) | 0.045 |
| O1 | 0.5017 (11) | 0.2075 (12) | 0.1637 (3) | 0.061 | C37 | 0.5391 (16) | −0.3206 (19) | 0.1433 (5) | 0.060 |
| O2 | 0.0826 (11) | 0.2138 (14) | 0.1015 (3) | 0.074 | C38 | 0.5994 (17) | −0.3940 (21) | 0.1310 (5) | 0.068 |
| O3 | 0.3720 (10) | −0.2276 (12) | 0.0728 (3) | 0.066 | C39 | 0.6806 (19) | −0.4061 (22) | 0.1453 (6) | 0.075 |
| O4 | 0.1813 (10) | 0.2146 (12) | 0.2057 (3) | 0.056 | C40 | 0.6970 (16) | −0.3592 (22) | 0.1720 (5) | 0.072 |
| O5 | 0.0728 (10) | −0.2260 (13) | 0.1111 (3) | 0.062 | C41 | 0.6343 (16) | −0.2929 (19) | 0.1838 (5) | 0.056 |
| O6 | 0.4905 (10) | −0.2028 (13) | 0.1819 (3) | 0.057 | O12 | 0.7517 (14) | 0.4744 (18) | 0.1360 (5) | 0.125 |
| C1 | 0.5662 (18) | 0.2364 (22) | 0.1856 (6) | 0.072 | C42 | 0.7474 (26) | −0.5044 (34) | 0.1099 (9) | 0.174 |
| C2 | 0.5715 (15) | 0.1828 (19) | 0.2139 (5) | 0.061 | N1 | 0.4010 (12) | 0.4998 (16) | 0.2274 (3) | 0.051 |
| C3 | 0.6389 (17) | 0.2068 (20) | 0.2325 (5) | 0.065 | C43 | 0.3742 (16) | 0.4172 (20) | 0.2024 (5) | 0.064 |
| C4 | 0.6997 (19) | 0.2872 (23) | 0.2271 (6) | 0.083 | C44 | 0.3965 (15) | 0.4604 (18) | 0.1696 (5) | 0.062 |
| C5 | 0.6958 (15) | 0.3487 (18) | 0.1999 (5) | 0.058 | C45 | 0.5036 (17) | 0.5020 (23) | 0.2292 (5) | 0.079 |
| C6 | 0.6251 (16) | 0.3235 (19) | 0.1795 (5) | 0.054 | C46 | 0.5410 (18) | 0.5747 (22) | 0.2560 (6) | 0.090 |
| O7 | 0.7663 (13) | 0.3194 (15) | 0.2489 (4) | 0.097 | C47 | 0.3609 (17) | 0.6092 (22) | 0.2227 (5) | 0.069 |
| C7 | 0.8379 (22) | 0.3892 (28) | 0.2420 (7) | 0.128 | C48 | 0.2621 (19) | 0.6142 (25) | 0.2168 (6) | 0.101 |
| C8 | 0.0222 (14) | 0.2208 (18) | 0.0783 (5) | 0.041 | C49 | 0.3629 (16) | 0.4493 (21) | 0.2564 (5) | 0.071 |
| C9 | −0.0483 (15) | 0.2963 (19) | 0.0788 (5) | 0.051 | C50 | 0.4001 (20) | 0.3372 (24) | 0.2660 (6) | 0.110 |
| C10 | −0.1082 (16) | 0.3135 (20) | 0.0534 (5) | 0.066 | N2 | 0.2577 (13) | 0.4767 (16) | 0.0556 (4) | 0.067 |
| C11 | −0.0917 (16) | 0.2439 (20) | 0.0270 (5) | 0.062 | C51 | 0.2970 (16) | 0.5538 (20) | 0.0315 (5) | 0.065 |
| C12 | −0.0232 (15) | 0.1741 (18) | 0.0251 (5) | 0.056 | C52 | 0.3455 (18) | 0.4931 (25) | 0.0062 (6) | 0.101 |
| C13 | 0.0341 (16) | 0.1584 (19) | 0.0519 (5) | 0.068 | C53 | 0.1877 (17) | 0.4025 (21) | 0.0422 (5) | 0.073 |
| O8 | −0.1590 (11) | 0.2610 (13) | 0.0031 (4) | 0.072 | C54 | 0.1039 (19) | 0.4574 (22) | 0.0266 (6) | 0.100 |
| C14 | −0.1410 (16) | 0.2031 (20) | −0.0248 (5) | 0.070 | C55 | 0.2204 (16) | 0.5558 (19) | 0.0797 (5) | 0.061 |
| C15 | 0.4279 (16) | −0.2091 (18) | 0.0492 (5) | 0.045 | C56 | 0.1761 (16) | 0.4993 (22) | 0.1060 (5) | 0.078 |
| C16 | 0.3915 (16) | −0.1586 (20) | 0.0242 (5) | 0.071 | C57 | 0.3304 (16) | 0.4005 (20) | 0.0707 (5) | 0.065 |
| C17 | 0.4433 (17) | −0.1551 (18 | −0.0030 (5) | 0.061 | C58 | 0.4092 (20) | 0.4604 (23) | 0.0846 (6) | 0.104 |
| C18 | 0.5296 (15) | −0.1874 (19) | −0.0023 (5) | 0.055 | N3 | 0.7711 (14) | 0.0333 (16) | 0.1343 (5) | 0.075 |
| C19 | 0.5678 (15) | −0.2367 (19) | 0.0244 (5) | 0.060 | C59 | 0.7817 (21) | −0.0606 (27) | 0.1120 (7) | 0.108 |
| C20 | 0.5138 (15) | −0.2402 (18) | 0.0495 (5) | 0.049 | C60 | 0.6964 (20) | −0.1306 (26) | 0.1067 (6) | 0.109 |
| O9 | 0.5894 (11) | −0.1867 (13) | −0.0267 (4) | 0.076 | C61 | 0.8600 (19) | 0.0918 (23) | 0.1346 (6) | 0.083 |
| C21 | 0.5547 (17) | −0.1235 (22) | −0.0532 (5) | 0.083 | C62 | 0.8691 (19) | 0.1893 (24) | 0.1571 (6) | 0.103 |
| C22 | 0.1274 (14) | 0.3043 (18) | 0.2025 (5) | 0.041 | C63 | 0.6900 (19) | 0.1094 (25) | 0.1243 (6) | 0.099 |
| C23 | 0.1079 (14) | 0.3673 (19) | 0.2287 (5) | 0.052 | C64 | 0.7011 (29) | 0.1582 (38) | 0.0930 (10) | 0.227 |
| C24 | 0.0556 (15) | 0.,4617 (18) | 0.2257 (5) | 0.055 | C65 | 0.7457 (21) | −0.0111 (29) | 0.1657 (7) | 0.117 |
| C25 | 0.0210 (16) | 0.5033 (23) | 0.1995 (5) | 0.068 | C66 | 0.8197 (28) | −0.0856 (34) | 0.1768 (8) | 0.183 |
| C26 | 0.0407 (15) | 0.4422 (19) | 0.1726 (5) | 0.058 | | | | | |

[a] Calculated standard deviations are indicated in parentheses.

## Results and Discussion

**Synthesis.** The new $[Fe_6S_6(p\text{-}RPhO)_6]^{3-}$ prismanes (R = MeO; $NMe_2$; COMe) can be obtained as described previously[19] for the *p*-Me analogue. The hydrolytic instability of these molecules becomes more pronounced with the highly electron-releasing −OMe and $-NMe_2$ para substituents. The synthesis of the $\{Fe_6S_6L_6[M(CO)_3]_2\}^{n-}$ adducts ($n$ = 3, 4) is accomplished readily by the reaction of the $(CH_3CN)_3M(CO)_3$ complexes with the $(Fe_6S_6L_6)^{3-}$ prismanes (eq 1).

$$[Fe_6S_6(ArO)_6]^{3-} + 2(CH_3CN)_3Mo(CO)_3 \rightarrow \{Fe_6S_6(ArO)_6[Mo(CO)_3]_2\}^{3-} \quad (1)$$

The complexes are extremely sensitive to oxygen and moisture and traces of moisture in the reaction mixture preclude the isolation of crystalline solids. The formation of the *p*-OMe prismane 2:1 adduct requires heating of the reaction mixture for 15 min at ~60 °C. No heating is required for the *p*-$NMe_2$ adduct which forms at ambient temperature within 15 min. This shows the enhanced reactivity of the phenoxy prismane with the *p*-$Me_2NPhO^-$ terminal ligands, which may be attributed to the exceptional electron-releasing characteristics of the *p*-$Me_2N$ group.

In addition to the need for anaerobic, moisture-free conditions in the synthesis, the isolation of pure $\{Fe_6S_6(ArO)_6[Mo(CO)_3]_2\}^{n-}$ adducts also depends on (a) the 3−/4− reduction potential of the $\{Fe_6S_6(ArO)_6[Mo(CO)_3]_2\}^{3-}$ clusters and (b) the relative stabilities of the 1:1 vs the 2:1 adducts. As discussed previously,[27] the $(CH_3CN)_3M(CO)_3$ reagents also can serve as reducing agents when the 3−/4− reduction potential of the $\{Fe_6S_6(ArO)_6[Mo(CO)_3]_2\}^{3-}$ adducts is more positive than −0.25 V. The 3−/4− redox couples for the $\{Fe_6S_6L_6[M(CO)_3]_2\}^{n-}$ clusters (L = *p*-$RPhO^-$) are greatly affected by the nature of the para substituents (vide infra). With electron-releasing R groups such as −Me or −OMe, the redox couples are found at potentials more negative than −0.25 V, and consequently, the trianionic adducts are obtained readily. With the electron-withdrawing −COMe as a para substituent, the 3−/4− couple is found at −0.16 V, and as a result, the 3− adduct can be reduced by the $(CH_3CN)_3M(CO)_3$ reagent. Under these circumstances, only the reduced tetraanionic adduct can be obtained in pure form, using an appropriate excess of $(CH_3CN)_3M(CO)_3$. A similar situation has been encountered in the synthesis of the $\{Fe_6S_6X_6[Mo(CO)_3]_2\}^{4-}$ adducts.[27] When stoichiometric amounts of $(CH_3CN)_3M(CO)_3$ are allowed to react with the $(Fe_6S_6L_6)^{3-}$ prismanes (L = *p*-$RPhO^-$, $Cl^-$, $Br^-$[27]), only

(27) Coucouvanis, D.; Salifoglou, A.; Kanatzidis, M. G.; Dunham, W. R.; Simopoulos, A.; Kostikas, A. *Inorg. Chem.* **1988**, *27*, 4066–4077.

**Table III.** Fractional Atomic Coordinates[a] and Equivalent Isotropic Thermal Parameters for the Non-Hydrogen Atoms in $(Et_4N)_3\{Fe_6S_6(p\text{-}OMePhO)_6[Mo(CO)_3]_2\}$ (II)

| atom | $x$ | $y$ | $z$ | $U$, Å$^2$ |
|---|---|---|---|---|
| Mo1 | −0.1653 (1) | −0.1815 (1) | −0.1215 (0) | 0.049 |
| Fe1 | 0.1021 (1) | −0.0513 (1) | −0.1178 (1) | 0.051 |
| Fe2 | −0.1336 (1) | 0.0551 (1) | −0.0701 (1) | 0.053 |
| Fe3 | −0.1120 (1) | −0.1647 (1) | 0.0743 (1) | 0.051 |
| S1 | −0.2344 (2) | −0.0942 (2) | 0.0164 (1) | 0.052 |
| S2 | 0.0026 (2) | −0.2017 (2) | −0.0316 (1) | 0.052 |
| S3 | −0.0197 (2) | 0.0178 (2) | −0.1752 (1) | 0.052 |
| O1 | 0.1864 (5) | −0.0878 (5) | −0.2060 (4) | 0.070 |
| O2 | −0.2347 (5) | 0.1031 (5) | −0.1263 (4) | 0.077 |
| O3 | −0.1852 (7) | −0.2952 (5) | 0.1338 (5) | 0.088 |
| CX1 | −0.1311 (9) | −0.2589 (9) | −0.2238 (8) | 0.081 |
| O7 | −0.1120 (8) | −0.3096 (8) | −0.2867 (6) | 0.135 |
| CX2 | −0.2832 (9) | −0.3283 (9) | −0.0888 (6) | 0.065 |
| O8 | −0.3574 (7) | −0.4168 (6) | −0.0712 (5) | 0.089 |
| CX3 | −0.2960 (9) | −0.1810 (8) | −0.1957 (6) | 0.065 |
| O9 | −0.3740 (6) | −0.1863 (6) | −0.2390 (5) | 0.097 |
| C1 | 0.2534 (8) | −0.0304 (9) | −0.2709 (7) | 0.064 |
| C2 | 0.2982 (9) | 0.0877 (10) | −0.2727 (6) | 0.074 |
| C3 | 0.3677 (9) | 0.1492 (9) | −0.3413 (8) | 0.081 |
| C4 | 0.3929 (9) | 0.0879 (13) | −0.4099 (8) | 0.092 |
| C5 | 0.3561 (13) | −0.0266 (12) | −0.4096 (8) | 0.112 |
| C6 | 0.2860 (11) | −0.0843 (9) | −0.3401 (8) | 0.100 |
| O4 | 0.4625 (10) | 0.1362 (9) | −0.4802 (7) | 0.145 |
| C7 | 0.4918 (20) | 0.2400 (28) | −0.4921 (15) | 0.301 |
| C8 | −0.2179 (9) | 0.1642 (9) | −0.1975 (7) | 0.074 |
| C9 | −0.1154 (10) | 0.2629 (11) | −0.2073 (8) | 0.090 |
| C10 | −0.1049 (12) | 0.3284 (10) | −0.2788 (10) | 0.110 |
| C11 | −0.1918 (16) | 0.2948 (14) | −0.3434 (10) | 0.121 |
| C12 | −0.2924 (14) | 0.1953 (16) | −0.3343 (10) | 0.132 |
| C13 | −0.3060 (10) | 0.1325 (10) | −0.2631 (8) | 0.094 |
| O5 | −0.1822 (14) | 0.3549 (14) | −0.4189 (9) | 0.235 |
| C14 | −0.1367 (45) | 0.4397 (34) | −0.4351 (24) | 0.569 |
| C15 | −0.2568 (9) | −0.3447 (7) | 0.1974 (7) | 0.058 |
| C16 | −0.3775 (11) | −0.4019 (9) | 0.1813 (7) | 0.080 |
| C17 | −0.4521 (9) | −0.4583 (10) | 0.2450 (9) | 0.082 |
| C18 | −0.4100 (11) | −0.4637 (10) | 0.3277 (8) | 0.083 |
| C19 | −0.2904 (12) | −0.4091 (11) | 0.3474 (7) | 0.095 |
| C20 | −0.2136 (8) | −0.3507 (9) | 0.2831 (8) | 0.073 |
| O6 | −0.4776 (9) | −0.5165 (9) | 0.3995 (6) | 0.131 |
| C21 | −0.6027 (15) | −0.5663 (13) | 0.3847 (10) | 0.140 |
| N1 | 0.6853 (7) | 0.2993 (6) | 0.0626 (6) | 0.078 |
| C22 | 0.6635 (8) | 0.1762 (8) | 0.0655 (7) | 0.077 |
| C23 | 0.5522 (10) | 0.1003 (9) | 0.1115 (8) | 0.094 |
| C24 | 0.7985 (9) | 0.3556 (8) | 0.0128 (9) | 0.097 |
| C25 | 0.8373 (11) | 0.4792 (10) | −0.0016 (12) | 0.148 |
| C26 | 0.6971 (14) | 0.3562 (11) | 0.1562 (12) | 0.131 |
| C27 | 0.7974 (20) | 0.3618 (12) | 0.2119 (12) | 0.167 |
| C28 | 0.5846 (10) | 0.3091 (10) | 0.0141 (11) | 0.113 |
| C29 | 0.5631 (11) | 0.2582 (11) | −0.0816 (12) | 0.131 |
| N2 | 0.0 (0) | 0.0 (0) | 0.5000 (0) | 0.101 |
| C30 | −0.0354 (22) | 0.0756 (21) | 0.4366 (16) | 0.109 |
| C31 | −0.0391 (22) | −0.1053 (20) | 0.4412 (15) | 0.099 |
| C32 | −0.0029 (18) | 0.1889 (17) | 0.4924 (14) | 0.202 |
| C33 | 0.1399 (23) | 0.0749 (21) | 0.5041 (18) | 0.118 |
| C34 | 0.0312 (23) | −0.0162 (21) | 0.4105 (16) | 0.104 |
| C35 | 0.1874 (16) | 0.0682 (15) | 0.4117 (12) | 0.173 |

[a] See footnote *a* in Table II.

**Table IV.** Fractional Atomic Coordinates[a] and Equivalent Isotropic Thermal Parameters for the Non-Hydrogen Atoms in $(Et_4N)_3\{Fe_6S_6(p\text{-}MePhO)_6[W(CO)_3]_2\}$ (III)

| atom | $x$ | $y$ | $z$ | $U$, Å$^2$ |
|---|---|---|---|---|
| W1 | 0.3578 (0) | 0.1719 (0) | 0.1336 (0) | 0.061 |
| Fe1 | 0.3766 (1) | −0.0379 (1) | −0.1163 (1) | 0.069 |
| Fe2 | 0.3702 (1) | −0.0521 (1) | 0.0758 (1) | 0.071 |
| Fe3 | 0.3775 (1) | 0.1681 (1) | −0.0693 (1) | 0.074 |
| S1 | 0.2595 (2) | 0.1019 (2) | −0.0057 (3) | 0.066 |
| S2 | 0.5135 (2) | 0.1935 (2) | 0.0356 (2) | 0.061 |
| S3 | 0.5052 (2) | −0.0277 (2) | 0.1792 (2) | 0.068 |
| O1 | 0.2758 (7) | −0.0630 (6) | −0.2074 (6) | 0.078 |
| O2 | 0.2663 (7) | −0.0927 (7) | 0.1310 (7) | 0.078 |
| O3 | 0.2833 (13) | 0.2952 (8) | −0.1278 (9) | 0.160 |
| O4 | 0.1699 (9) | 0.4170 (8) | 0.0945 (9) | 0.108 |
| O5 | 0.4526 (9) | 0.2709 (9) | 0.3065 (8) | 0.100 |
| O6 | 0.1582 (9) | 0.1800 (9) | 0.2590 (8) | 0.103 |
| C1 | 0.2171 (9) | −0.0046 (9) | −0.2822 (9) | 0.061 |
| C2 | 0.1729 (10) | 0.1090 (9) | −0.2818 (8) | 0.056 |
| C3 | 0.1116 (10) | 0.1644 (10) | −0.3596 (9) | 0.060 |
| C4 | 0.0921 (10) | 0.1129 (10) | −0.4393 (9) | 0.061 |
| C5 | 0.1356 (12) | −0.0009 (12) | −0.4400 (11) | 0.094 |
| C6 | 0.1971 (13) | −0.0583 (10) | −0.3622 (12) | 0.102 |
| C7 | 0.0231 (12) | 0.1776 (12) | −0.5227 (10) | 0.092 |
| C8 | 0.2802 (9) | −0.1729 (9) | 0.1858 (9) | 0.057 |
| C9 | 0.1861 (11) | −0.1567 (12) | 0.2426 (10) | 0.074 |
| C10 | 0.1992 (14) | −0.2394 (17) | 0.2979 (12) | 0.113 |
| C11 | 0.2967 (18) | −0.3402 (15) | 0.2972 (13) | 0.117 |
| C12 | 0.3924 (13) | −0.3555 (11) | 0.2431 (12) | 0.094 |
| C13 | 0.3825 (12) | −0.2701 (11) | 0.1899 (11) | 0.088 |
| C14 | 0.3109 (22) | −0.4318 (20) | 0.3564 (19) | 0.207 |
| C15 | 0.2318 (9) | 0.3489 (8) | −0.1988 (7) | 0.044 |
| C16 | 0.8903 (15) | −0.4108 (13) | 0.1932 (10) | 0.095 |
| C17 | 0.9430 (16) | −0.4838 (15) | 0.3084 (12) | 0.113 |
| C18 | 0.8423 (14) | −0.4562 (13) | 0.3534 (10) | 0.088 |
| C19 | 0.7231 (19) | −0.3842 (18) | 0.3158 (15) | 0.143 |
| C20 | 0.6756 (19) | −0.3338 (18) | 0.2466 (15) | 0.049 |
| C21 | 0.8577 (33) | −0.5253 (32) | 0.4474 (26) | 0.122 |
| C20′ | 0.9913 (27) | −0.4592 (25) | 0.2318 (20) | 0.088 |
| C21′ | 1.0740 (27) | −0.5653 (26) | 0.3803 (20) | 0.092 |
| C22 | 0.2412 (12) | 0.3243 (11) | 0.1091 (10) | 0.078 |
| C23 | 0.4179 (13) | 0.2353 (11) | 0.2434 (10) | 0.079 |
| C24 | 0.2340 (12) | 0.1738 (10) | 0.2108 (15) | 0.099 |
| N1 | 0.8241 (7) | 0.2997 (7) | 0.0801 (7) | 0.063 |
| C25 | 0.9250 (9) | 0.3152 (10) | 0.0444 (9) | 0.062 |
| C26 | 0.9464 (14) | 0.2868 (13) | −0.0582 (10) | 0.085 |
| C27 | 0.8466 (9) | 0.1783 (8) | 0.0686 (9) | 0.063 |
| C28 | 0.9598 (11) | 0.0944 (10) | 0.1128 (10) | 0.073 |
| C29 | 0.8118 (16) | 0.3407 (11) | 0.1835 (12) | 0.115 |
| C30 | 0.7141 (27) | 0.3324 (13) | 0.2316 (20) | 0.240 |
| C31 | 0.7060 (11) | 0.3662 (10) | 0.0285 (13) | 0.097 |
| C32 | 0.6608 (12) | 0.4915 (11) | 0.0321 (14) | 0.109 |
| N2 | 0.5000 (0) | 0.0 (0) | 0.5000 (0) | 0.056 |
| C33 | 0.4051 (19) | −0.0574 (18) | 0.5060 (15) | 0.054 |
| C34 | 0.3775 (27) | −0.1037 (27) | 0.4117 (22) | 0.081 |
| C35 | 0.6167 (21) | −0.0949 (20) | 0.4583 (16) | 0.064 |
| C36 | 0.6745 (25) | −0.2035 (24) | 0.5106 (22) | 0.053 |
| C37 | 0.4461 (24) | 0.0881 (23) | 0.4413 (19) | 0.076 |
| C38 | 0.3187 (30) | 0.1798 (29) | 0.4726 (24) | 0.076 |
| C39 | 0.4839 (20) | −0.0222 (19) | 0.3952 (15) | 0.055 |
| C40 | 0.3842 (25) | −0.0694 (25) | 0.3835 (21) | 0.070 |

[a] See footnote *a* in Table II.

mixtures of the 1:1 and 2:1 adducts are obtained. The use of an excess of the $(CH_3CN)_3M(CO)_3$ reagent therefore is necessary for the isolation of pure 2:1 adducts free of 1:1 contaminants.

The octanuclear $Mo(CO)_3$ adducts can be obtained not only by using the preformed $Fe_6S_6$ units but also through the reorganization of smaller units. The reaction of either the dinuclear $[Fe_2S_2(ArO)_4]^{2-}$ or the tetranuclear $[Fe_4S_4(ArO)_4]^{2-}$ clusters in acetonitrile with $(CH_3CN)_3Mo(CO)_3$ affords the octanuclear clusters in an excellent yield (eqs 2 and 3). The possible function

$$3[Fe_2S_2(ArO)_4]^{2-} + 5(CH_3CN)_3Mo(CO)_3 \rightarrow \{Fe_6S_6(ArO)_6[Mo(CO)_3]_2\}^{3-,4-} \quad (2)$$

$$3[Fe_4S_4(ArO)_4]^{2-} + 4(CH_3CN)_3Mo(CO)_3 \rightarrow \{Fe_6S_6(ArO)_6[Mo(CO)_3]_2\}^{3-,4-} \quad (3)$$

of the $M(CO)_3$ units as templates, for the assembly of $(Fe_2S_2L_2)^-$ fragments, has been discussed previously.[27]

The purity of the adducts can be monitored by examination of the infrared spectra in the C≡O stretching frequency region. The presence of more than two strong, sharp vibrations in this region usually is diagnostic of mixtures. The *p*-Me and *p*-OMe 4− prismane adducts are obtained cleanly in reductions of the corresponding trianions with $(Et_4N)BH_4$ in $CH_3CN$ solution.

**Description of Structures.** In all structures of the $Et_4N^+$ cations well separated from the anions and are unexceptional. Mean values and ranges for the C–N and C–C bond lengths in the $Et_4N^+$ cations are tabulated in a footnote in Table VI. All three prismane adducts, II–IV, crystallize in the triclinic space group $P\bar{1}$. Each of the three triclinic unit cells contain one anion that is required

**Table V.** Fractional Atomic Coordinates[a] and Equivalent Isotropic Thermal Parameters for the Non-Hydrogen Atoms in $(Et_4N)_4\{Fe_6S_6(p\text{-}COMePhO)_6[Mo(CO)_3]_2\}$ (IV)

| atom | *x* | *y* | *z* | *U*, Å$^2$ |
|---|---|---|---|---|
| Mo1 | 0.2712 (1) | 0.2972 (1) | 0.4010 (1) | 0.050 |
| Fe1 | 0.3468 (1) | 0.5521 (1) | 0.4211 (1) | 0.050 |
| Fe2 | 0.4005 (1) | 0.3740 (1) | 0.5724 (1) | 0.050 |
| Fe3 | 0.5462 (1) | 0.3976 (1) | 0.4172 (1) | 0.050 |
| S1 | 0.4693 (3) | 0.2841 (2) | 0.4991 (2) | 0.049 |
| S2 | 0.4142 (3) | 0.4658 (3) | 0.3454 (2) | 0.049 |
| S3 | 0.2666 (3) | 0.4431 (3) | 0.5032 (2) | 0.049 |
| CX1 | 0.1174 (14) | 0.2901 (12) | 0.3250 (8) | 0.071 |
| O7 | 0.0250 (10) | 0.2799 (10) | 0.2809 (7) | 0.121 |
| CX2 | 0.1627 (12) | 0.1715 (12) | 0.4336 (7) | 0.064 |
| O8 | 0.0873 (9) | 0.0870 (8) | 0.4487 (6) | 0.088 |
| CX3 | 0.2608 (14) | 0.1839 (12) | 0.3243 (8) | 0.064 |
| O9 | 0.2506 (11) | 0.1124 (9) | 0.2792 (6) | 0.102 |
| O1 | 0.2206 (7) | 0.5893 (7) | 0.3577 (5) | 0.069 |
| C1 | 0.2178 (13) | 0.6459 (12) | 0.3041 (8) | 0.061 |
| C2 | 0.3244 (13) | 0.7399 (14) | 0.2985 (8) | 0.074 |
| C3 | 0.3157 (13) | 0.8018 (12) | 0.2418 (9) | 0.076 |
| C4 | 0.2003 (18) | 0.7736 (14) | 0.1856 (9) | 0.087 |
| C5 | 0.0925 (15) | 0.6821 (15) | 0.1894 (9) | 0.084 |
| C6 | 0.0989 (13) | 0.6192 (12) | 0.2454 (8) | 0.076 |
| C7 | 0.1984 (22) | 0.8445 (19) | 0.1246 (13) | 0.142 |
| O4 | 0.0918 (16) | 0.8158 (14) | 0.0761 (9) | 0.190 |
| C8 | 0.3054 (19) | 0.9456 (17) | 0.1218 (11) | 0.138 |
| O2 | 0.3061 (8) | 0.2731 (7) | 0.6278 (5) | 0.077 |
| C9 | 0.3109 (15) | 0.205 (14) | 0.6747 (10) | 0.071 |
| C10 | 0.2023 (15) | 0.1259 (15) | 0.6822 (10) | 0.114 |
| C11 | 0.2007 (17) | 0.0619 (15) | 0.7413 (11) | 0.107 |
| C12 | 0.3084 (24) | 0.0949 (17) | 0.8001 (12) | 0.131 |
| C13 | 0.4224 (21) | 0.1949 (19) | 0.8020 (12) | 0.133 |
| C14 | 0.4187 (17) | 0.2543 (14) | 0.7426 (11) | 0.107 |
| C15 | 0.3227 (26) | 0.0342 (22) | 0.8648 (15) | 0.166 |
| O5 | 0.4289 (20) | 0.0567 (17) | 0.9132 (11) | 0.242 |
| C16 | 0.2115 (26) | −0.0580 (23) | 0.8688 (14) | 0.204 |
| O3 | 0.5800 (7) | 0.3126 (7) | 0.3461 (5) | 0.069 |
| C17 | 0.6153 (11) | 0.3348 (12) | 0.2866 (8) | 0.058 |
| C18 | 0.5897 (13) | 0.2391 (12) | 0.2312 (9) | 0.083 |
| C19 | 0.6290 (15) | 0.2599 (14) | 0.1708 (9) | 0.094 |
| C20 | 0.6940 (13) | 0.3694 (15) | 0.1586 (8) | 0.075 |
| C21 | 0.7153 (12) | 0.4626 (12) | 0.2104 (9) | 0.067 |
| C22 | 0.6760 (11) | 0.4447 (12) | 0.2733 (8) | 0.060 |
| C23 | 0.7362 (17) | 0.3926 (17) | 0.0915 (10) | 0.104 |
| O6 | 0.7795 (12) | 0.4910 (12) | 0.0787 (7) | 0.132 |
| C24 | 0.7313 (24) | 0.2966 (21) | 0.0396 (12) | 0.221 |
| N1 | 0.1785 (9) | 0.8159 (8) | 0.5054 (6) | 0.064 |
| C25 | 0.1837 (12) | 0.7100 (12) | 0.5316 (9) | 0.091 |
| C26 | 0.1044 (14) | 0.6590 (15) | 0.5828 (11) | 0.123 |
| C27 | 0.0438 (12) | 0.7907 (12) | 0.4594 (8) | 0.076 |
| C28 | −0.0213 (13) | 0.7002 (13) | 0.3878 (9) | 0.093 |
| C29 | 0.2284 (14) | 0.9130 (13) | 0.5708 (9) | 0.092 |
| C30 | 0.3631 (15) | 0.9580 (14) | 0.6207 (10) | 0.107 |
| C31 | 0.2623 (13) | 0.8492 (12) | 0.4571 (9) | 0.094 |
| C32 | 0.2714 (16) | 0.9519 (4) | 0.4225 (11) | 0.133 |
| N2 | 0.2535 (13) | 0.3284 (13) | 0.0845 (8) | 0.108 |
| C33 | 0.1642 (18) | 0.3787 (17) | 0.0707 (9) | 0.137 |
| C34 | 0.1580 (21) | 0.4352 (19) | 0.1385 (13) | 0.164 |
| C35 | 0.3894 (18) | 0.4191 (19) | 0.1316 (10) | 0.127 |
| C36 | 0.4416 (23) | 0.5202 (22) | 0.0935 (14) | 0.184 |
| C37 | 0.2444 (17) | 0.2865 (17) | 0.0058 (11) | 0.135 |
| C38 | 0.3331 (26) | 0.2288 (23) | 0.0018 (15) | 0.221 |
| C39 | 0.2224 (20) | 0.2368 (19) | 0.1305 (11) | 0.152 |
| C40 | 0.0951 (24) | 0.1378 (21) | 0.0939 (13) | 0.178 |

[a] See footnote *a* in Table II.

by space group symmetry to reside on a crystallographic inversion center. The three adducts are quite similar, and all contain the $Fe_6S_6$ prismane core. The $Fe_3S_3$ hexagonal cross sections of this core have a "chair" conformation and serve as tridentate ligands for $Mo(CO)_3$ structural subunits in II and IV and for $W(CO)_3$ subunits in III. The centrosymmetric octanuclear $M_2Fe_6S_6$ core, which forms following the addition of the $M(CO)_3$ fragments to a $Fe_6S_6$ unit, show a distorted $M_2Fe_6$ cube with a $\mu_4$-$S^{2-}$ ligand occupying a position above the center of each of the six faces. The rhombic dodecahedral core ($D_{3d}$ symmetry) also is found in the pentlandite type of solids such as $Co_9S_8$[28] and $(Ni,Fe)_9S_8$[29] and in molecular clusters such as $[Co_8S_6(SPh)_8]^{4-}$ [30] and $[Fe_8S_6I_8]^{3-}$ [31] and has been described previously.[27] The structural details of the adducts reported in this paper (Table VI) resemble closely those of the haloprismane adducts that have been described in detail previously.[27] Particular features that must be reemphasized include the following. (a) The $Fe_6S_6$ cores in the aryloxy prismane adducts are elongated along the idealized $\bar{6}$ axis, relative to the cores in the parent prismanes. (b) The Mo–Fe and Mo–S distances in the trianionic (oxidized) adducts are slightly shorter than those of the tetraanionic adducts. (c) The Fe–Fe distances in either the hexagonal or rhombic faces of the $Fe_6S_6$ cores in the adducts are similar to those in the parent prismanes. The Mo–S distances in the aryloxy adducts are slightly longer than those in the halo analogues and perhaps indicate a more oxidized Mo and a more reduced $Fe_6S_6$ core in the halo adducts. This finds support in the Mossbauer spectra of the adducts (vide infra).

**Electronic Structure.** Systematic changes in the electronic structures of the $Fe_6S_6$ cores, brought about by the addition of the $M(CO)_3$ units, are evident in comparative spectroscopic studies of the parent prismanes and their adducts. The origin of these changes can be probed further by analyzing the pronounced substituent effects observed when para-substituted phenoxide ligands are used as terminal ligands for the $Fe_6S_6$ prismanes.

**Mössbauer Spectra.** The Mössbauer isomer shift (IS) values for the new para-substituted $[Fe_6S_6(p\text{-}RPhO)_6]^{3-}$ clusters (Table VII) are similar to those reported previously for other similar clusters and can be regarded as characteristic for $(Fe_6S_6)^{3+}$ cores, with phenoxide terminal ligands and the iron atoms in a +2.5 formal oxidation state. An increase in the electron-releasing strength of the para substituents in the $[Fe_6S_6(p\text{-}RPhO)_6]^{3-}$ clusters correlates with a slight increase in the Mössbauer IS values and may indicate a slight increase of electron density in the $Fe_6S_6$ cores. The significance of this correlation is only marginal in view of the fact that no such correlation is detected in the Mössbauer spectra of the $\{Fe_6S_6(p\text{-}RPhO)_6[Mo(CO)_3]_2\}^{3-,4-}$ clusters.

The IS values of the $\{Fe_6S_6(p\text{-}RPhO)_6[Mo(CO)_3]_2\}^{3-}$ clusters are (Table VII) smaller than those of the $\{Fe_6S_6L_6[Mo(CO)_3]_2\}^{3-}$ halo analogues[27] (L = Cl, Br, I). Similar differences in IS values, which are attributed to differences in the type of terminal ligands, already have been found for the $(Fe_4S_4L_4)^{2-}$ cubanes[32] and the $(Fe_2S_2L_4)^{2-}$ dimers.[33]

The IS values of the $[Fe_6S_6(p\text{-}RPhO)_6[Mo(CO)_3]_2]^{3-}$ clusters are significantly greater than those of the corresponding $[Fe_6S_6(p\text{-}RPhO)_6]^{3-}$ "parent" prismanes and indicate that in the former the average formal oxidation state of the Fe atoms is lower than that in the latter. The apparent partial reduction of the $Fe_6S_6$ cores in the $\{Fe_6S_6(p\text{-}RPhO)_6[Mo(CO)_3]_2\}^{3-}$ clusters is possible only with a concomitant partial oxidation of the Mo atoms in the $Mo(CO)_3$ units and may well be due to direct Mo→Fe charge transfer.

The $\{Fe_6S_6(p\text{-}RPhO)_6[Mo(CO)_3]_2\}^{4-}$ clusters, obtained by reduction of the corresponding trianions, show IS values that are greater than those of the trianions by ~0.07 mm/s. As discussed previously,[27] a change in the oxidation level of the $Fe_6S_6$ core by a unit charge would be expected to change the $^{57}$Fe IS values approximately by (1/6)0.45 or 0.075 mm/s. The observed changes suggest that in the reduced aryloxy adducts a significant portion of the added charge resides in the $Fe_6S_6$ cores. Unexpectedly, the implied reduction in the average Fe oxidation level in the tetraanionic adducts is not evident in significant structural differences in the $Fe_6S_6$ cores of the $\{Fe_6S_6(p\text{-}RPhO)_6[Mo(CO)_3]_2\}^{n-}$

(28) Rajamani, V.; Prewitt, C. T. *Can. Mineral.* **1975**, *13*, 75.
(29) Rajamani, V.; Prewitt, C. T. *Can. Mineral.* **1973**, *12*, 178.
(30) Christou, G.; Hagen, K. S.; Bashkin, J. K.; Holm, R. H. *Inorg. Chem.* **1985**, *24*, 1010.
(31) Pohl, S.; Saak, W. *Angew. Chem., Int. Ed. Engl.* **1984**, *23*, 907.
(32) Kanatzidis, M. G.; Coucouvanis, D.; Simopoulos, A.; Kostikas, A.; Papaefthymiou, V. *J. Am. Chem. Soc.* **1985**, *107*, 4925.
(33) (a) Salifoglou, A.; Simopoulos, A.; Kostikas, A.; Dunham, R. W.; Kanatzidis, M. G.; Coucouvanis, D. *Inorg. Chem.* **1988**, *27*, 3394. (b) Salifoglou, A. Ph.D. Thesis, The University of Michigan, Ann Arbor, MI, 1987.

**Table VI.** Summary of Interatomic Distances (Å) and Angles (deg) for $(Et_4N)_3[Fe_6S_6(p\text{-}OMePhO)_6]$ (I), $(Et_4N)_3[Fe_6S_6(p\text{-}OMePhO)_6[Mo(CO)_3]_2]$ (II), $(Et_4N)_3[Fe_6S_6(p\text{-}MePhO)_6[W(CO)_3]_2]$ (III), and $(Et_4N)_4[Fe_6S_6(p\text{-}COMePhO)_6[Mo(CO)_3]_2]$ (IV)

| | I | II | III | IV |
|---|---|---|---|---|
| | | Distances[a,b] | | |
| Mo(W)–Fe[a] | | 2.99 (2, 3) | 2.96 (2, 3) | 3.00 (2, 3) |
| range | | 2.954 (1)–3.028 (1) | 2.931 (2)–2.976 (2) | 2.969 (2)–3.016 (2) |
| Mo(W)–S | | 2.614 (5, 3) | 2.590 (3, 3) | 2.646 (8, 3) |
| range | | 2.605 (2)–2.619 (2) | 2.589 (3)–2.590 (3) | 2.639 (3)–2.659 (3) |
| Mo(W)–C | | 1.94 (2, 3) | 1.97 (3, 3) | 1.92 (3, 3) |
| range | | 1.92 (1)–1.98 (1) | 1.94 (1)–2.01 (1) | 1.88 (1)–1.96 (1) |
| Fe–Fe(eq)[c] | 3.829 (9, 6) | 3.82 (1, 3) | 3.806 (9, 3) | 3.78 (2, 3) |
| range | 3.806 (5)–3.863 (5) | 3.797 (2)–3.835 (2) | 3.794 (2)–3.820 (3) | 3.754 (2)–3.815 (2) |
| Fe–Fe(ax)[c] | 2.78 (1, 6) | 2.80 (2, 3) | 2.791 (3, 3) | 2.79 (2, 3) |
| range | 2.752 (5)–2.825 (5) | 2.779 (2)–2.823 (2) | 2.786 (3)–2.796 (3) | 2.746 (2)–2.789 (2) |
| Fe–S(eq) | 2.289 (7, 12) | 2.291 (4, 6) | 2.284 (4, 6) | 2.288 (4, 6) |
| range | 2.267 (7)–2.320 (7) | 2.282 (2)–2.304 (2) | 2.273 (4)–2.297 (4) | 2.275 (3)–2.301 (3) |
| Fe–S(ax) | 2.309 (7, 6) | 2.341 (3, 3) | 2.338 (6, 3) | 2.348 (4, 3) |
| range | 2.302 (6)–2.315 (7) | 2.339 (3)–2.342 (3) | 2.331 (3)–2.348 (3) | 2.341 (3)–2.352 (3) |
| S–S(eq) | 3.80 (2, 6) | 3.88 (5, 6) | 3.82 (2, 6) | 3.85 (3, 6) |
| range | 3.736 (8)–3.843 (8) | 3.821 (3)–3.971 (3) | 3.790 (4)–3.844 (5) | 3.813 (4)–3.884 (4) |
| S–S(ax) | 3.66 (2, 6) | 3.69 (5, 3) | 3.684 (4, 3) | 3.71 (3, 3) |
| range | 3.613 (8)–3.699 (8) | 3.667 (2)–3.709 (2) | 3.681 (4)–3.689 (4) | 3.675 (4)–3.745 (4) |
| Fe–O | 1.87 (1, 6) | 1.85 (1, 3) | 1.85 (1, 3) | 1.912 (8, 3) |
| range | 1.85 (2)–1.89 (2) | 1.831 (7)–1.866 (6) | 1.830 (8)–1.858 (9) | 1.911 (8)–1.915 (8) |
| O–C(Ph) | 1.34 (2, 6) | 1.32 (1, 3) | 1.31 (4, 3) | 1.27 (2, 3) |
| range | 1.30 (2)–1.38 (3) | 1.30 (1)–1.33 (1) | 1.24 (1)–1.36 (1) | 1.26 (2)–1.30 (1) |
| | | Angles | | |
| Fe–Mo(W)–Fe | | 79.5 (1, 3) | 80.2 (1, 3) | 78.3 (3, 3) |
| range | | 79.3 (1)–79.6 (1) | 80.1 (1)–80.2 (1) | 77.8 (1)–78.6 (1) |
| S–Mo(W)–S | | 94.1 (9, 3) | 94.9 (6, 3) | 93.4 (6, 3) |
| | | 92.8 (1)–95.3 (1) | 94.0 (1)–95.8 (1) | 92.5 (1)–94.3 (1) |
| Fe–Fe–Fe(eq) | 60.0 (2, 6) | 60.0 (4, 3) | 60.0 (2, 3) | 60.0 (6, 3) |
| range | 59.3 (1)–60.6 (1) | 59.4 (1)–60.4 (1) | 59.7 (1)–60.4 (1) | 59.3 (1)–60.9 (1) |
| Fe–S–Fe(eq) | 113.6 (6, 6) | 112.9 (8, 3) | 112.8 (8, 3) | 111.4 (9, 3) |
| range | 112.1 (3)–115.4 (3) | 111.7 (1)–114.1 (1) | 111.7 (1)–114.0 (2) | 110.1 (1)–112.8 (1) |
| Fe–S–Fe(ax) | 74.5 (3, 12) | 74.4 (3, 6) | 74.3 (1, 6) | 73.8 (5, 6) |
| range | 72.9 (2)–76.1 (6) | 73.5 (1)–75.2 (1) | 73.9 (1)–74.6 (1) | 72.4 (1)–75.2 (1) |
| S–Fe–S(eq) | 112.3 (5, 6) | 113.2 (7, 3) | 113.2 (4, 3) | 114.6 (8, 3) |
| range | 110.2 (3)–113.4 (3) | 112.1 (1)–114.0 (1) | 112.7 (1)–114.0 (1) | 113.7 (1)–115.8 (1) |
| S–Fe–S(ax) | 105.5 (3, 12) | 105.6 (3, 6) | 105.7 (1, 6) | 106.2 (5, 6) |
| range | 103.9 (2)–106.9 (2) | 104.8 (1)–106.5 (1) | 105.4 (1)–105.9 (1) | 105.0 (1)–107.8 (3) |
| O–Fe–S(eq) | 110.8 (10, 12) | 111 (1, 6) | 111.1 (5, 6) | 109 (1, 6) |
| range | 106.6 (5)–118.0 (5) | 106.0 (1)–116.0 (1) | 109.5 (2)–112.9 (3) | 105.1 (1)–112.3 (1) |
| O–Fe–S(ax) | 112 (2, 6) | 109.4 (4, 3) | 109.7 (4, 3) | 112.3 (4, 3) |
| range | 111.7 (5)–116.7 (5) | 108.9 (1)–110.0 (1) | 109.1 (2)–110.2 (2) | 111.8 (1)–112.9 (1) |
| Fe–O–C(Ph) | 133 (3, 6) | 136.3 (7, 3) | 140 (9, 3) | 138 (5, 3) |
| range | 129 (1)–143 (2) | 129.9 (6)–146.1 (7) | 130.3 (9)–153.9 (9) | 133.4 (8)–146 (1) |

[a] Mean values of crystallographically independent, chemically equivalent, structural parameters. The number in parentheses represents the larger of the individual standard deviations or the standard deviation from the mean: $\sigma = [\sum_{i=1}^{N}(x_i - \bar{x})^2/N(N-1)]^{1/2}$. [b] In I: For cation N1 the N–C bonds are in the range 1.53 (3)–1.45 (3) Å with a mean value of 1.51 (4) Å. The C–C bonds are in the range 1.58 (3)–1.47 (3) Å with a mean of 1.53 (5) Å. For cation N2, the N–C bonds are in the range 1.54 (3)–1.47 (3) Å with a mean of 1.52 (3) Å. The C–C bonds are within the range 1.54 (3)–1.48 (3) Å with a mean value of 1.51 (3) Å. The Cation N3 shows the N–C bonds within the range 1.56 (3)–1.49 (3) Å with a mean value of 1.52 (3) and the C–C bonds in the range 1.54 (3)–1.48 (4) Å with a mean value of 1.51 (3) Å. In II: For cation N1 the N–C bonds are within the range 1.510 (11) to 1.506 (11) Å with a mean value of 1.51 (1) Å. The C–C bonds are within the range 1.51 (1)–1.48 (2) Å with a mean value of 1.50 (1) Å. For the disordered cation N2, the N–C bonds are within the range 1.60 (2)–1.46 (2) Å with a mean value of 1.5 (1) Å. The C–C bonds range from 1.53 (3)–1.51 (3) Å with a mean value of 1.52 (3) Å. For III: Cation N1, N–C range = 1.48 (2)–1.53 (2) Å, mean N–C = 1.51 (2) Å, C–C range = 1.48 (4)–1.51 (2) Å, mean C–C = 1.50 (4) Å; disordered cation N2, N–C range = 1.40 (3)–1.68 (3) Å, mean N–C = 1.56 (6) Å, C–C range = 1.53 (4)–1.62 (5) Å, mean C–C = 1.56 (5) Å. For IV: Cation N1, N–C range = 1.51 (1)–1.49 (1) Å, mean = 1.50 (1) Å, C–C range = 1.53 (2)–1.48 (2) Å, mean C–C = 1.50 (2) Å; cation N2, C–N range = 1.53 (2)–1.47 (2) Å, mean N–C = 1.49 (2) Å, C–C range = 1.57 (3)–1.46 (2) Å, mean C–C = 1.50 (5) Å. [c] The designations ax (axial) and eq (equatorial) are with reference to the idealized 6-fold axis in the structures of the anions. Distances or angles designated "equatorial" are found within the two hexagonal $Fe_3S_3$ structural subunits. Those designated as "axial" are found within the six rhombic $Fe_2S_2$ subunits.

adducts ($n = 3$ vs $n = 4$). Instead, the reduction affects significantly the $Mo(CO)_3$ units. A partial reduction of the $Mo(CO)_3$ units is evident in longer Mo–S and Mo–Fe distances (Table VI) and in lower C–O vibrational frequencies (vide infra) in the reduced, tetraanionic, (aryloxy)prismane adducts. Similar effects have been observed previously with the haloprismane adducts.[27] It appears that, in the reduction of the 3– prismane adducts, the added electron enters an antibonding molecular orbital that has considerable Mo, Fe, and S character.

**Electronic Spectra.** As indicated above (Table VII), Mössbauer spectroscopy is rather insensitive to small perturbations in the electronic structure of the (aryloxy)prismanes and adducts. In contrast, the prismane clusters and their adducts show electronic absorptions in the visible and infrared regions of the spectrum (Table VIII) that are very sensitive to phenyl ring-substituent effects.

The O→Fe charge-transfer absorptions are found at lower energies as the electron-releasing effect of the para substituents

**Table VII.** $^{57}$Fe Mössbauer Parameters for $[Fe_6S_6(p\text{-}XPhO)_6\{Mo(CO)_3\}_2]^{n-}$, $[Fe_6S_6(p\text{-}XPhO)_6]^{3-}$ ($n$ = 3, X = Me, OMe, $NMe_2$; $n$ = 4, X = Me, OMe, COMe), and $(Et_4N)_3\{Fe_6S_6(p\text{-}MePhO)_6[W(CO)_3]_2\}$

| cluster | temp, K | IS ($\delta$), mm/s | $\Delta Eq$, mm/s |
|---|---|---|---|
| $(Et_4N)_3\{Fe_6S_6(p\text{-}MeOPh)_6[Mo(CO)_3]_2\}$ | 125 | 0.532 | 0.845 |
| $(Et_4N)_3\{Fe_6S_6(p\text{-}OMeOPh)_6[Mo(CO)_3]_2\}$ | 125 | 0.551 | 0.800 |
| $(Et_4N)_3\{Fe_6S_6(p\text{-}NMe_2OPh)_6[Mo(CO)_3]_2\}$ | 125 | 0.544 | 0.739 |
| $(Et_4N)_4\{Fe_6S_6(p\text{-}MeOPh)_6[Mo(CO)_3]_2\}$ | 125 | 0.60 | 1.04 |
| $(Et_4N)_4\{Fe_6S_6(p\text{-}OMeOPh)_6[Mo(CO)_3]_2\}$ | 125 | 0.616 | 0.867 |
| $(Et_4N)_4\{Fe_6S_6(p\text{-}COMeOPh)_6[Mo(CO)_3]_2\}$ | 125 | 0.620 | 1.02 |
| $(Et_4N)_3\{Fe_6S_6(p\text{-}MeOPh)_6[W(CO)_3]_2\}$ | 125 | 0.581 | 0.74 |
| $(Et_4N)_3[Fe_6S_6(p\text{-}MeOPh)_6]$ | 125 | 0.477 | 1.016 |
| $(Et_4N)_3[Fe_6S_6(p\text{-}OMeOPh)]$ | 125 | 0.496 | 1.016 |
| $(Et_4N)_3[Fe_6S_6(p\text{-}NMe_2OPh)_6]$ | 125 | 0.512 | 0.979 |

increases from –COMe to –Me to $-NMe_2$. In comparison to the corresponding parent prismanes, the 3– prismane adducts show a bathochromic shift in the O→Fe charge-transfer absorption by ~40 nm. It seems that addition of the $Mo(CO)_3$ units to the prismanes indirectly lowers the energy of the O→Fe charge transfer by withdrawing $\pi$-electron density from the $\mu_3$-S donor atoms. In the spectra of the 4– adducts, a hypsochromic shift of the O→Fe charge transfer by 30–40 nm is observed by comparison to the 3– adducts (Table VIII). This electronic effect is as expected since, in the 4– adducts, partial reduction of the Mo atoms will weaken the $\mu_2$-S–Mo $\pi$ bonding and at the same time strengthen the $\mu_2$-S–Fe $\pi$ bonding. The net result will be a weakening of O–Fe $\pi$ bonding that leads to the hypsochromic shift of the O→Fe charge-transfer bands in the 4– adducts.

**Infrared Spectra.** As expected for the $C_{3v}$ local symmetry of the $M(CO)_3$ units in the prismane adducts, two sharp C–O vibrations ($A_1$ + E) are observed in the infrared spectra between 1915 and 1800 cm$^{-1}$. These are 20–30 cm$^{-1}$ lower in energy than the C–O doublets in the IR spectra of the (1,4,7-trithiacyclononane)$Mo(CO)_3$,[34,35] $(Et_2S)_3Mo(CO)_3$,[36] $(C_4H_8S)_3Mo(CO)_3$,[36] and $(Ph_3P)_3Mo(CO)_3$[37] complexes. In the far-IR spectra of the (aryloxy)prismane adducts, two medium-intensity bands in the 450–480-cm$^{-1}$ region are assigned to the Mo–C $A_1$ and E stretching vibrations. The frequencies of these vibrations for the W adduct (462 and 480 cm$^{-1}$) are higher than those of the corresponding Mo complex (457 and 474 cm$^{-1}$). Similar differences in energies of the M–C vibrations in $M(CO)_3$ units (Mo vs W) have been reported previously for Mo and W $\eta^6$-benzene[38] and mesitylene complexes.[38] These differences follow the reverse order observed for the difference in frequencies of the carbonyl stretching vibrations ($\nu_{CO}$(Mo) > $\nu_{CO}$(W) and are due to the lower oxidation potential of W(0) compared to Mo(0).

In the $\{Fe_6S_6(p\text{-}RPhO)_6[M(CO)_3]_2\}^{n-}$ adducts ($n$ = 3, 4), the C–O frequencies are found 30–40 cm$^{-1}$ lower in energy than those for corresponding halo complexes. It seems that the Mo atoms in the haloprismane adducts are less "electron rich" than the corresponding aryloxy clusters. The greater partial reduction of the Mo atoms in the aryloxy clusters is due to more effective O→$Fe_6S_6$→Mo charge transfer through $\pi$ bonding and also is apparent in the lower values for the isomer shifts (and more oxidized Fe atoms) in these clusters.

The reduced, 4–, aryloxy adducts show the C–O vibrations 40–50 cm$^{-1}$ lower in energy than those for the corresponding 3– adducts and suggest more reduced Mo atoms in the former. This also is evident in crystallographically determined structural differences (Mo–S distances) between the 3– and 4–adducts (vide supra). The C–O stretching frequencies in the (aryloxy)prismane adducts are affected by the type of the phenyl para substituents and are found at lower energies with the more electron-releasing substituents. Apparently, an excess of electron density is transmitted to the Mo atom and the C–O $\pi^*$ orbitals by a pathway already described. The common origin of the changes in the electronic and infrared spectra, in the type of para substituent, is evident in nearly linear correlations between the CT absorption energies in the electronic spectra and the C–O vibrational frequencies (Table VIII).

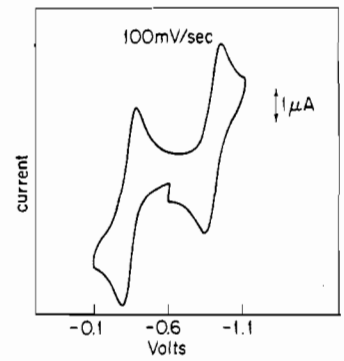


**Figure 3.** Cyclic voltammetric trace of $(Et_4N)_3\{Fe_6S_6(p\text{-}EtPhO)_6[M(CO)_3]_2\}$ in $CH_2Cl_2$ solution. Qualitatively similar waves are obtained for other members of the $\{Fe_6S_6(p\text{-}RPhO)_6[M(CO)_3]_2\}^{n-}$ series.

In the absence of an excess of $(CH_3CN)_3Mo(CO)_3$ the product obtained in the synthesis of II shows an additional doublet of C=O absorptions at 1880 and 1800 cm$^{-1}$. An examination of the latter product by proton NMR spectroscopy (vide infra) shows two sets of isotropically shifted resonances for the *o*-, *m*-, and *p*-$CH_3$ protons. One set consists of singlets and is due to the $\{Fe_6S_6(p\text{-}MePhO)_6[Mo(CO)_3]_2\}^{3-}$ 2:1 adduct. The other set consists of doublets and is tentatively assigned to the $\{Fe_6S_6(p\text{-}MePhO)_6[Mo(CO)_3]\}^{3-}$ 1:1 adduct.

**Electrochemical Measurements.** The cyclic voltammetry of the adducts was studied in $CH_2Cl_2$ solution on a Pt electrode with $(Bu_4N)ClO_4$ as supporting electrolyte. The $\{Fe_6S_6(p\text{-}RPhO)_6[Mo(CO)_3]_2\}^{3-,4-}$ clusters show two one-electron reversible waves (Figure 3) in cyclic voltammetry that correspond to the 3–/4– and 4–/5– redox couples. An irreversible cathodic wave also is observed around –1.50 V. A multielectron irreversible oxidation is observed for the (aryloxy)prismane adducts at potentials centered around +0.25 V. The products of this oxidative degradation have not been characterized to date.

The potential of the first of the two voltammetric waves (Table IX) is significantly affected by the nature of the para substituents on the aryloxy ligands. With electron-releasing groups, such as –Me, –OMe, and $-NMe_2$, the redox couple is found (vide infra) at potentials more negative than –0.25 V. With the electron-withdrawing –COMe, the 3–/4– couple is found at a potential low enough (–0.16 V) to allow for the chemical reduction of the 3– adduct by $(CH_3CN)_3Mo(CO)_3$. This accounts for the formation of the $\{Fe_6S_6(p\text{-}COMePhO)_6[M(CO)_3]_2\}^{4-}$ adduct in a procedure that with other (electron releasing) substituents affords only the 3– adducts. Addition of the appropriate stoichiometric amount of arenethiols to solutions of the $\{Fe_6S_6(p\text{-}RPhO)_6[Mo(CO)_3]_2\}^{3-}$ clusters generates in situ the corresponding arenethiolate adducts. The chemically unstable $\{Fe_6S_6(PhS)_6[Mo(CO)_3]_2\}^{3-}$ adduct obtained in this fashion shows two one-electron reversible waves with $E_{1/2}$ values of –0.25 and –0.70 V. Slightly more positive redox potentials for the thiophenolate analogues also have been detected previously for the $[Fe_6S_6(PhX)_6]^{3-}$ prismanes and the $[Fe_4S_4(PhX)_4]^{2-}$ cubanes (X = O, S).

Substitution of Mo by W slightly shifts the redox couple of the first wave to more negative potentials. Similar shifts have been encountered previously in the double cubane clusters[14] and the $[(PhS)_2FeS_2MS_2]^{2-}$ and $[(S_5)_2FeS_2MS_2]^{2-}$ complexes.[13]

**Proton NMR Spectra.** The high-spin tetrahedral Fe centers in the $\{Fe_6S_6(p\text{-}RPhO)_6[M(CO)_3]_2\}^{3-,4-}$ (M = Mo, W) clusters are antiferromagnetically coupled. The trianions are characterized by an $S = {}^1/_2$ spin ground state and their EPR spectra that can be obtained only at a temperature <15 K resemble those of the

(34) Ashby, M. T.; Lichtenberger, D. L. *Inorg. Chem.* **1985**, *24*, 636–638.
(35) Backes-Dahmann, G.; Wieghardt, K. *Inorg. Chem.* **1985**, *24*, 4049–4054.
(36) Cotton, F. A.; Zingales, F. *Inorg. Chem.* **1962**, *1*, 145.
(37) Abel, E. W.; Bennett, M. A.; Wilkinson, G. *J. Chem. Soc.* **1959**, 2323.
(38) Kettle, S. F. A. The Vibrational Spectra of Metal Carbonyls. *Top. Curr. Chem.* **1977**, *71*, 112.

**Table VIII.** Infrared and UV/Visible Electronic Spectral Data for $\{Fe_6S_6(p\text{-}XPhO)_6[Mo(CO)_3]_2\}^{n-}$, $[Fe_6S_6(p\text{-}XPhO)_6]^{3-}$ ($n$ = 3, X = Me, OMe, $NMe_2$; $n$ = 4, X = Me, OMe, COMe), and $(Et_4N)_3\{Fe_6S_6(p\text{-}MePhO)_6[W(CO)_3]_2\}$ in $CH_3CN$ Solution

| cluster | $\nu_{CO}$, $cm^{-1}$ | $\nu MC$, $cm^{-1}$ | $\lambda$, nm | $\epsilon$, $M^{-1}$ $cm^{-1}$ |
|---|---|---|---|---|
| $(Et_4N)_3\{Fe_6S_6(p\text{-}MePhO)_6[Mo(CO)_3]_2\}$ | 1916, 1865 | 474, 457 | 468 | 18 130 |
| $(Et_4N)_3\{Fe_6S_6(p\text{-}OMePhO)_6[Mo(CO)_3]_2\}$ | 1911, 1854 | 477, 469 | 480 | 17 410 |
| $(Et_4N)_3\{Fe_6S_6(p\text{-}NMe_2PhO)_6[Mo(CO)_3]_2\}$ | 1909, 1854 | 479, 461 | 520 | 18 750 |
| $(Et_4N)_4\{Fe_6S_6(p\text{-}MePhO)_6[Mo(CO)_3]_2\}$ | 1885, 1805 | 483, 460 | 426 | 15 670 |
| $(Et_4N)_4\{Fe_6S_6(p\text{-}OMePhO)_6[Mo(CO)_3]_2\}$ | 1882, 1797 | 485, 461 | 420 | 14 990 |
| $(Et_4N)_4\{Fe_6S_6(p\text{-}COMePhO)_6[Mo(CO)_3]_2\}$ | 1897, 1832 | 477, 459 | 436 | 14 530 |
| $(Et_4N)_3\{Fe_6S_6(p\text{-}MePhO)_6[W(CO)_3]_2\}$ | 1909, 1855 | 480, 462 | 470 | 20 320 |
| $(Et_4N)_3[Fe_6S_6(p\text{-}MePhO)_6]$ | | | 427 | 19 720 |
| $(Et_4N)_3[Fe_6S_6(p\text{-}OMePhO)_6]$ | | | 443 | 17 280 |
| $(Et_4N)_3[Fe_6S_6(p\text{-}NMe_2PhO)_6]$ | | | 490 | 19 330 |

**Table IX.** Cyclic Voltammetry Data[a] for the $Et_4N^+$ Salts of the $\{Fe_6S_6(p\text{-}XPhO)_6[Mo(CO)_3]_2\}^{n-}$, $[Fe_6S_6(p\text{-}XPhO)_6]^{3-}$[b] ($n$ = 3, X = Me, OMe, $NMe_2$; $n$ = 4, X = Me, OMe, COMe), and $\{Fe_6S_6(p\text{-}MePhO)_6[W(CO)_3]_2\}^{3-}$ Anions in $CH_2Cl_2$ Solution[c]

| cluster | 3−/4− $E_{1/2}$, mV | $\Delta E$, mV | $i_{pa}/i_{pc}$ | 4−/5− $E_{1/2}$, mV | $\Delta E$, mV | $i_{pa}/i_{pc}$ |
|---|---|---|---|---|---|---|
| $(Et_4N)_3\{Fe_6S_6(p\text{-}MePhO)_6[Mo(CO)_3]_2\}$ | −0.29 | 110 | 1.0 | −0.87 | 103 | 0.96 |
| $(Et_4N)_3\{Fe_6S_6(p\text{-}OMePhO)_6[Mo(CO)_3]_2\}$ | −0.31 | 130 | 1.0 | −0.87 | 130 | 0.93 |
| $(Et_4N)_3\{Fe_6S_6(p\text{-}NMe_2PhO)_6[Mo(CO)_3]_2\}$ | −0.40 | 110 | 0.96 | −0.91 | 110 | 0.93 |
| $(Et_4N)_4\{Fe_6S_6(p\text{-}COMePhO)_6[Mo(CO)_3]_2\}$ | −0.16 | 100 | 0.90 | −0.67 | 130 | 0.96 |
| $(Et_4N)_3\{Fe_6S_6(p\text{-}MePhO)_6[W(CO)_3]_2\}$ | −0.38 | 141 | 0.96 | −0.87 | 130 | 0.96 |
| $(Et_4N)_3[Fe_6S_6(p\text{-}OMePhO)_6]$ | −0.22 | 110 | 0.96 | −1.17 | 160 | 0.85 |
| $(Et_4N)_3[Fe_6S_6(p\text{-}NMe_2PhO)_6]$ | −0.32 | 150 | 0.96 | −1.27 | 170 | 0.85 |

[a] For all measurements, the scan rate was 200 mV/s. [b] The first potential refers to the 2−/3− redox couple and the second potential refers to the 3−/4− one. [c] The potentials are reported vs SCE. Normally, the $(Et_4N)^+$ salts of the above clusters are not soluble in $CH_2Cl_2$. In the presence of excess $(n\text{-}Bu_4N)ClO_4$ as supporting electrolyte, they readily go into solution.

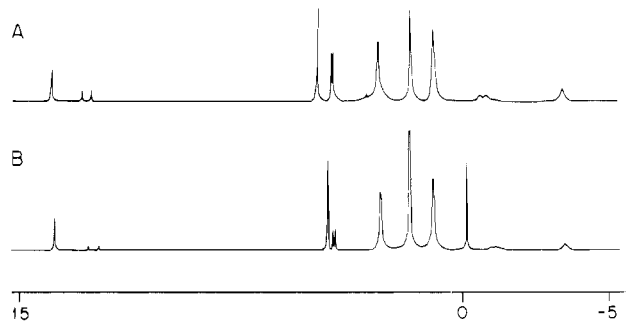


**Figure 4.** $^1H$ NMR spectra (ppm) of the $Et_4N^+$ salts of the $\{Fe_6S_6(p\text{-}RPhO)_6[Mo(CO)_3]_2\}^{3-}$ clusters in $CD_3CN$ solution: (A) R = $-NMe_2$; (B) R = −OMe.

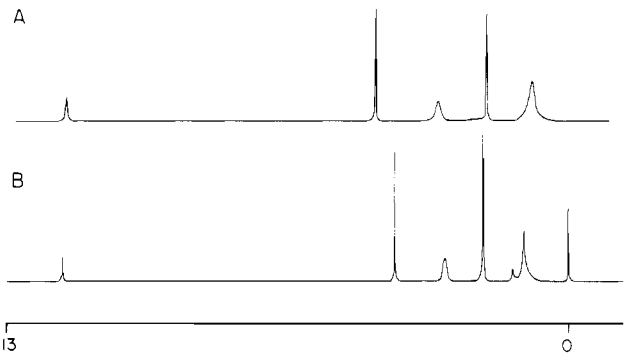


**Figure 5.** $^1H$ NMR spectra (ppm) of the $Et_4N^+$ salts of the $[Fe_6S_6(p\text{-}RPhO)_6]^{3-}$ prismanes in $CD_3CN$ solution: (A) R = $-NMe_2$; (B) R = −OMe.

$[Fe_6S_6(ArO)_6]^{3-}$ prismanes. The corresponding tetraanions are EPR silent and possess an integer spin state.

The $^1H$ NMR spectra of the (aryloxy)prismane adducts (Figure 4) have been measured in deuterated acetonitrile solutions at room temperature. In addition to the resonances due to the tetraethylammonium cations, isotropically shifted resonances due to the phenoxide protons also are observed. The room-temperature resonances in ppm are given in Table X. The pattern of alternating signs of the isotropic shifts of the aryl proton resonances is similar to those observed for $[Fe_2S_2(ArO)_4]^{2-}$,[39] $[Fe_4S_4(ArO)_4]^{2-}$,[40] and $[Fe_6S_6(ArO)_6]^{3-}$[19] and is typical for M−X−Ar (X = S, O, Se) paramagnetic complexes. It has been attributed previously to dominant Fermi contact interactions ($\pi$ delocalization mechanism), with negligible pseudocontact contributions.[41]

The ortho proton resonances are shifted to higher fields (relative to the diamagnetic phenoxy phenol) while the meta protons are shifted to lower fields. The ortho proton resonances, as observed previously in the aryloxy $Fe_6S_6$ prismanes, the $Fe_4S_4$ cubanes, and the $Fe_2S_2$ dimers, are identified by their relative broadness that is due to electronic spin relaxation effects, induced by their proximity to the paramagnetic centers.

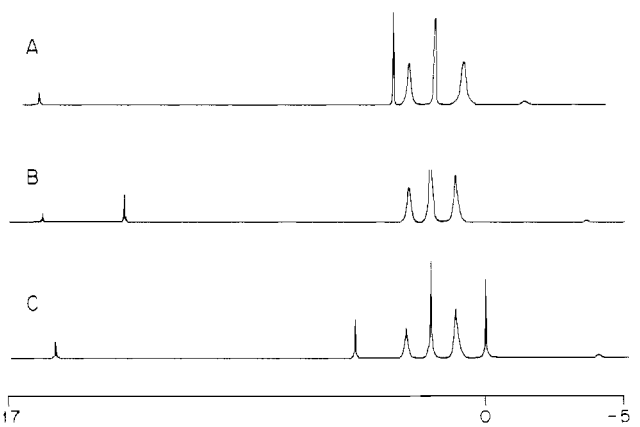


**Figure 6.** $^1H$ NMR spectra (ppm) of the $Et_4N^+$ salts of the $\{Fe_6S_6(p\text{-}RPhO)_6[Mo(CO)_3]_2\}^{4-}$ clusters in $CD_3CN$ solution: (A) R = −COMe; (B) R = −Me; (C) R = −OMe.

The isotropic shifts observed for the (aryloxy)prismane adducts are greater in magnitude than those of the $[Fe_6S_6(ArO)_6]^{3-}$ parent prismanes (Figure 5), the $[Fe_2S_2(ArO)_4]^{2-}$ dimers, or the $[Fe_4S_4(ArO)_4]^{2-}$ clusters. This observation suggests that there is more contact between the ring protons and the paramagnetic centers in the $Fe_6S_6$ cores of the adducts, and accordingly may

(39) (a) Coucouvanis, D.; Salifoglou, A.; Kanatzidis, M. G.; Simopoulos, A.; Papaefthymiou, V. *J. Am. Chem. Soc.* **1984**, *106*, 6081. (b) Cleland, W. E.; Averill, B. A. *Inorg. Chem.* **1984**, *23*, 4192.
(40) Cleland, W. E.; Holtman, D. A.; Sabat, M.; Ibers, J. A.; Defotis, G. C.; Averill, B. A. *J. Am. Chem. Soc.* **1983**, *105*, 6021.
(41) (a) Holm, R. H.; Phillips, W. D.; Averill, B. A.; Mayerle, J. J.; Herskovitz, T. *J. Am. Chem. Soc.* **1974**, *96*, 2109. (b) Reynolds, J. G.; Laskowski, E. J.; Holm, R. H. *J. Am. Chem. Soc.* **1978**, *100*, 5315.

**Table X.** $^1$H NMR Spectral Data for the $Et_4N^+$ salts of the $\{Fe_6S_6(p\text{-}RPhO)_6[Mo(CO)_3]_2\}^{n-}$, $[Fe_6S_6(p\text{-}RPhO)_6]^{3-}$ [b] ($n$ = 3, R = Me, OMe, $NMe_2$; $n$ = 4, R = Me, OMe, COMe), and $\{Fe_6S_6(p\text{-}MePhO)_6[W(CO)_3]^2\}$ Anions in $CD_3CN$ Solution

| cluster | chem shift, ppm ($(\Delta H/H_0)_{iso}$)[a] | | |
|---|---|---|---|
| | *o*-H | *m*-H | *p*-R |
| $(Et_4N)_3\{Fe_6S_6(p\text{-}MePhO)_6[Mo(CO)_3]_2\}$ | −3.0 (9.8) | 14.47 (−7.67) | 1.8 (−9.55) |
| $(Et_4N)_3\{Fe_6S_6(p\text{-}OMePhO)_6[Mo(CO)_3]_2\}$ | −3.38 (10.12) | 13.97 (−7.23) | 4.69 (−0.97) |
| | −1.00, −0.97 | 12.77, 12.43 | 4.49, 4.45 |
| $(Et_4N)_3\{Fe_6S_6(p\text{-}NMe_2PhO)_6[Mo(CO)_3]_2\}$ | −3.06 (9.71) | 14.06 (−7.41) | 5.0 (−2.3) |
| | −1.05, −1.10[b] | 12.82, 12.51[b] | 4.39, 4.35[b] |
| $(Et_4N)_4\{Fe_6S_6(p\text{-}MePhO)_6[Mo(CO)_3]_2\}$ | −3.56 (10.36) | 15.76 (−8.96) | 12.86 (−10.61) |
| $(Et_4N)_4\{Fe_6S_6(p\text{-}OMePhO)_6[Mo(CO)_3]_2\}$ | −4.03 (10.77) | 15.29 (−8.55) | 4.72 (−1.0) |
| $(Et_4N)_4\{Fe_6S_6(p\text{-}COMePhO)_6[Mo(CO)_3]_2\}$ | −0.55 (7.91) | 15.55 (−8.19) | 3.27 (−0.79) |
| $(Et_4N)_3\{Fe_6S_6(p\text{-}MePhO)_6[W(CO)_3]_2\}$ | −3.42 (10.22) | 14.79 (−7.99) | 12.31 (−10.06) |
| $(Et_4N)_3[Fe_6S_6(p\text{-}MePhO)_6]$ | 1.28 (5.52) | 12.0 (−5.2) | 8.32 (−6.07) |
| $(Et_4N)_3[Fe_6S_6(p\text{-}OMePhO)_6]$ | 1.32 (5.42) | 11.62 (−4.88) | 4.33 (−0.61) |
| $(Et_4N)_3[Fe_6S_6(p\text{-}NMe_2PhO)_6]$ | 1.25 (5.4) | 11.75 (−5.1) | 4.05 (−1.35) |

[a] $(\Delta H/H_0)_{iso} = (\Delta H/H_0)_{diam} - (\Delta H/H_0)_{obsd}$ measured in $CD_3CN$ solution at room temperature. Shifts vs diamagnetic references: $p$-$CH_3C_6H_4OH$, 6.8, 2.25 ppm ($CH_3$); $p$-$CH_3OC_6H_4OH$, 6.74, 3.72 ppm ($CH_3$), $p$-$CH_3COC_6H_4OH$, 7.36, 2.48 ppm ($CH_3$), $p$-$N(CH_3)_2C_6H_4OH$, 6.65, 2.7 ppm ($CH_3$). [b] Resonances (ppm) due to the $\{Fe_6S_6(p\text{-}RPhO)_6[Mo(CO)_3]\}^{3-}$ 1:1 adducts.

indicate that the Fe···O bond in the latter has more covalent character than that in the parent prismanes.

By comparison to the trianionic adducts that have an $S = {}^1/_2$ ground state, the tetraanionic adducts (with an integer spin ground state), at NMR probe temperatures (ca. 37 °C), show (Figure 6) even larger shifts than the trianionic adducts. Thus in $(Et_4N)_3\{Fe_6S_6(p\text{-}OMePhO)_6[Mo(CO)_3]_2\}$ the *o*-H, *m*-H and *p*-OMe proton signals are observed at −3.38, 13.97, and 4.69 ppm, respectively. In the tetraanionic adduct, those resonances are observed at −4.03, 15.29, and 4.72 ppm.

The *o*-H, *m*-H, and *p*-$CH_3$ signals in the $\{Fe_6S_6(p\text{-}MePhO)_6[Mo(CO)_3]_2\}^{3-}$ adduct at −3.00, 14.47, and 11.88 ppm correspond to isotropic shifts of 9.80, −7.67, and −9.55 ppm. The low-field shift of the *p*-Me resonance is consistent with the assumption that $\pi$-electron spin density at that position leads to a direct contact interaction with the methyl protons through hyperconjugation. Similar arguments can be advanced to explain the isotropic shifts observed in the *p*-OMe and *p*-$NMe_2$ substituents.

For each resonance observed for the *o*-H, *m*-H, and *p*-R protons, an additional minor set of resonances (doublets) is present in the spectra of the 3− $Mo(CO)_3$ aryloxide adducts (Figure 4). The relative intensity of this set of doublets increases upon addition of $[Fe_6S_6(p\text{-}RPhO)_6]^{3-}$, and decreases upon addition of $(CH_3CN)_3Mo(CO)_3$. These observations are consistent with the equilibrium

$$\{Fe_6S_6(p\text{-}RPhO)_6[M(CO)_3]_2\}^{3-} + 3CD_3CN \rightarrow \{Fe_6S_6(p\text{-}RPhO)_6[M(CO)_3]\}^{3-} + (CD_3CN)_3Mo(CO)_3 \quad (4)$$

and suggest that the set of doublets in the spectra are due to the 3− 1:1 adduct. Upon prolonged standing, resonances that can be attributed to traces of free prismane also appear and indicate the equilibrium

$$\{Fe_6S_6(p\text{-}RPhO)_6[M(CO)_3]\}^{3-} + 3CD_3CN \rightarrow [Fe_6S_6(p\text{-}RPhO)_6]^{3-} + (CD_3CN)_3Mo(CO)_3 \quad (5)$$

With strongly electron-releasing para substituents, such as −OMe and −$NMe_2$, the intensity of the doublet signals that arise from the 1:1 adducts is nearly twice that of the 2:1 adducts and the equilibrium (eq 4) lies to the right. Indeed the synthesis of pure 1:1 adducts should be possible in noncoordinating solvents, in stoichiometric reactions between the $[Fe_6S_6(p\text{-}RPhO)_6]^{3-}$ prismanes (R = −OMe and −$NMe_2$) and $(CH_3CN)_3Mo(CO)_3$. The $^1$H NMR spectra of the tetraanionic $Mo(CO)_3$ adducts or of the trianionic $W(CO)_3$ adduct do not show dissociation of $M(CO)_3$.

## Summary and Conclusions

As with the haloprismane adducts reported previously, the (aryloxy)prismane adducts reported herein possess a Mo:Fe stoichiometry of 1:3, magnetic ground states $S = {}^1/_2$ and $S$ = integer for the 3− and 4− levels, respectively, and structural features that only qualitatively resemble the Fe/Mo/S site in nitrogenase. The ultimate purpose of our synthetic studies, to isolate 1:1 prismane adducts with Mo in high (3+ or 4+) oxidation states, and a Fe:Mo ratio of at least 6:1 still remains to be achieved. Nevertheless, this work has revealed certain aspects of Fe/Mo/S chemistry that are expected to be very useful in future synthetic studies. It is now clear that the fine details of charge distribution in the (aryloxy)prismanes and their $M(CO)_3$ adducts are determined by remote substituent effects. These details can be monitored by electronic spectroscopy. The O→Fe charge-transfer absorptions in the electronic spectra of the parent prismanes and of the $M(CO)_3$ adducts shift to lower energies as the electron-releasing strength of the para substituents on the phenoxy ligands increases. In the $M(CO)_3$ adducts, the frequencies of the C–O stretching vibrations also are affected predictably by the electron-releasing characteristics of the para substituents. In general, the greater the electron-releasing strength of the para substituent, the lower the frequency of the C–O vibration.

Crystallographic and Mössbauer spectroscopic studies on the (aryloxy)prismane adducts reenforce the conclusions reached earlier[27] in studies of the analogous haloprismane adducts. These were as follows. (a) The $Fe_6S_6$ cores in the adducts have undergone partial reduction when compared to the cores in the parent prismanes. (b) Oxidation–reduction of the adducts is centered primarily on the Mo atoms. The properties of the clusters reported herein show that with electron-releasing phenyl para substituents, the 1:1 (aryloxy)prismane adducts are stable and may be isolated under appropriate conditions.

The unrealistically low oxidation state of the Mo atom is another major objectionable feature of the $Mo(CO)_3$ prismane adducts. A 4+ formal oxidation state has been proposed for the Mo atom in nitrogenase, on the basis of ENDOR studies.[42] A high oxidation state, (3+, 4+), for the Mo atom also is supported by the Mo–S bond lengths (~2.35 Å) derived from Mo EXAFS analyses.[9] Preliminary studies, on oxidative decarbonylation reactions of $\{Fe_6S_6Cl_6[M(CO)_3]_2\}^{3-}$, have shown that such reactions are feasible with quinones. The product of the reaction with tetrachloro-*o*-quinone[43] however is not a prismane adduct, but rather the known $[MoFe_3S_4Cl_3(Cl_4cat)(CH_3CN)]^{2-}$ cubane with the $[MoFe_3S_4]^{3+}$ core.[14] The latter may well be a reorganization product of a $\{Fe_6S_6Cl_6[Mo(Cl_4cat)L]_2\}^{-}$ adduct that forms initially. The stability of such adducts may depend greatly on the nature of the terminal ligands on the $Fe_6S_6$ cores. The $Fe_6S_6$ prismanes are metastable clusters relative to the $Fe_4S_4$ cubanes, particularly when the iron atoms are coordinated by terminal halide or thiophenolate ligands. The stability of the $Fe_6S_6$ prismanes increases dramatically however with aryloxide terminal ligands. At present, we are directing our efforts toward the synthesis of 1:1 (aryl-

(42) Venters, R. A.; Nelson, M. J.; McLean, P. A.; True, A. E.; Levy, M. A.; Hoffman, B. M.; Orme-Johnson, W. H. *J. Am. Chem. Soc.* **1986**, *108*, 3487.
(43) Al-Ahmad, S. S.; Coucouvanis, D. Work in progress.

oxy)prismane adducts with $Mo(CO)_3$ and on the oxidative decarbonylation of these compounds with quinones or alkyl peroxides.

**Acknowledgment.** The support of this work by a grant (GM-26671) from the National Institutes of Health is gratefully acknowledged.

**Supplementary Material Available:** Listings of positional and thermal parameters for $(Et_4N)_3[Fe_6S_6(p\text{-}OMePhO)_3]$ (I), $(Et_4N)_3\{Fe_6S_6(p\text{-}OMePhO)_6[Mo(CO)_3]_2\}$ (II), $(Et_4N)_3\{Fe_6S_6(p\text{-}MePhO)_6[W(CO)_3]_2\}$ (III), and $(Et_4N)_4\{Fe_6S_6(p\text{-}COMePhO)_6[Mo(CO)_3]_2\}$ (IV) (Tables S1-S4) (55 pages); listings of structure factors (Tables S5-S8) (57 pages). Ordering information is given on any current masthead page.

Contribution from the Lehrstuhl für Anorganische Chemie I der Ruhr-Universität, D-4630 Bochum, FRG, and Anorganisch-Chemisches Institut der Universität, D-6900 Heidelberg, FRG

# Synthesis and Coordination Chemistry of the Hexadentate Ligands 1,4,7-Tris(2-hydroxybenzyl)-1,4,7-triazacyclononane ($H_3L^1$) and 1,4,7-Tris(3-*tert*-butyl-2-hydroxybenzyl)-1,4,7-triazacyclononane ($H_3L^2$). Crystal Structures of $[HL^1Cu^{II}]$ and $[L^2Fe^{III}]$acacH

Ulf Auerbach,[1a] Uwe Eckert,[1a] Karl Wieghardt,*[,1a] Bernhard Nuber,[1b] and Johannes Weiss[1b]

*Received June 7, 1989*

Two new hexadentate macrocycles containing phenolate pendant arms have been prepared from 1,4,7-triazacyclononane and 3 equiv of 2-(bromomethyl)phenyl acetate: 1,4,7-tris(2-hydroxybenzyl)-1,4,7-triazacyclononane ($H_3L^1$; $C_{27}H_{33}N_3O_3$) and 1,4,7-tris(3-*tert*-butyl-2-hydroxybenzyl)-1,4,7-triazacyclononane ($H_3L^2$, $C_{39}H_{57}N_3O_3$). The reaction of trivalent first-row transition metals with the trianions affords monomeric pseudooctahedral complexes, of which the following have been characterized: $L^1Mn^{III}$; $L^1Fe^{III}$; $L^2Co^{III}$; $[L^2Fe^{III}]$acacH; $L^2Fe^{III}$; $L^2Mn^{III}$. The reaction of copper(II) perchlorate with the new ligands affords five-coordinate species: $HL^1Cu^{II}$; $[H_2L^2Cu^{II}]ClO_4$ (green), $[HL^2Cu^{II}]NaClO_4$ (red). $Co(BF_4)_2{\cdot}6H_2O$ reacts with $H_3L^1$ in the presence of air to give a trinuclear complex: $[(L^1Co^{III})_2Co^{II}](BF_4)_2{\cdot}H_2O$. The crystal structures of $[HL^1Cu^{II}]$ (**1**) and $[L^2Fe^{III}]$acacH (**2**), where acacH is acetylacetone, have been determined by X-ray crystallography: (**1**) space group $P2_1/n$, $a$ = 8.687 (4) Å, $b$ = 13.320 (9) Å, $c$ = 20.789 (8) Å, $\beta$ = 102.09 (4)°, $Z$ = 4; (**2**) space group $P2_1/n$, $a$ = 12.347 (9) Å, $b$ = 18.929 (9) Å, $c$ = 17.699 (9) Å, $\beta$ = 92.23 (6)°, $Z$ = 4. In **1** the Cu(II) center is in a square-based-pyramidal environment of three nitrogen donors and two phenolate oxygen atoms whereas the ferric ion in **2** is in a pseudooctahedral environment ($N_3O_3$ donor set). Electronic spectral data, magnetic properties, and the electrochemistry of the new complexes are reported.

## Introduction

In recent years the tridentate, facially coordinating macrocycle 1,4,7-triazacyclononane has been repeatedly N-functionalized and a series of potentially hexadentate ligands have been synthesized and their coordination chemistry investigated.[2,3] Chart I summarizes these ligands. In this paper we present two new such ligands, which contain phenolate pendant arms. Recently, Moore and co-workers[4] have reported the first ligand of this kind, namely 1,4,7-tris(3,5-dimethyl-2-hydroxybenzyl)-1,4,7-triazacyclononane, which was shown to form a stable gallium(III) complex. This work prompted us to publish our own results now. We had independently synthesized 1,4,7-tris(2-hydroxybenzyl)-1,4,7-triazacyclononane ($H_3L^1$) and 1,4,7-tris(3-*tert*-butyl-2-hydroxybenzyl)-1,4,7-triazacyclononane ($H_3L^2$) and studied their coordination chemistry with first-row transition metals such as Fe(III), Mn(III), Co(III), and Cu(II).

## Experimental Section

The ligand 1,4,7-triazacyclononane (tacn) was prepared according to published procedures.[5] All other chemicals were obtained from commercial sources and used as received.

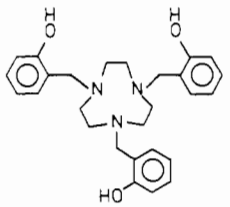

$H_3L^1$

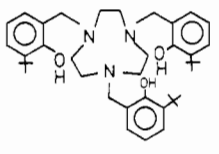

$H_3L^2$

*Caution!* Perchlorate salts of metal complexes with organic ligands are potentially explosive. Only small quantities of these should be handled behind suitable protective shields.

**Synthesis of 1,4,7-Tris(2-hydroxybenzyl)-1,4,7-triazacyclononane ($H_3L^1$).** To a solution of dry, finely powdered KOH (3.90 g; 66 mmol) in toluene (30 mL) was added 1,4,7-triazacyclononane (1.29 g; 10 mmol). To this solution was added dropwise a toluene solution (20 mL) of 2-(bromomethyl)phenyl acetate[6] (6.87 g; 30 mmol) at 0 °C. The combined solutions were stirred at room temperature for 12 h. The precipitated KBr was filtered off, and the solvent was removed by evaporation under reduced pressure. To the resulting orange oil was added 0.1 M NaOH (100 mL), and the solution was stirred at 20 °C for 3 h, after which time the product was extracted from the aqueous phase with $CH_2Cl_2$ (three times with 50 mL). The combined organic phases were dried over $MgSO_4$. After removal of the solvent by rotary evaporation a colorless solid was obtained in 20-30% yield with respect to 1,4,7-triazacyclononane.

$^1H$ NMR ($CDCl_3$; $\delta$): 6.71-7.22 (m, 12 H, phenyl), 3.74 (s, 6 H, N-$CH_2$-R), 2.79 (s, 12 H, N-$CH_2CH_2$-N). The phenolic protons were not observed. $^{13}C$ NMR (20 °C, $CDCl_3$; $\delta$): 157.3, 129.2, 129.1, 122.0, 119.4, 116.1, 62.6, 55.7. MS: $m/z$ 447. UV-vis ($CH_3CN$; $\lambda_{max}$, nm ($\epsilon$, L mol$^{-1}$ cm$^{-1}$)): 275 (2400), 280 (sh).

The colorless trisodium salt, $Na_3L^1$, was prepared from sodium methanolate and $H_3L^1$ (3:1) dissolved in dry methanol followed by rotary evaporation of the solvent under reduced pressure. UV-vis ($CH_3CN$;

(1) (a) Ruhr-Universität Bochum. (b) Universität Heidelberg.
(2) Chaudhuri, P.; Wieghardt, K. *Prog. Inorg. Chem.* **1987**, *35*, 329.
(3) (a) Arishima, T.; Hamada, K.; Takamoto, S. *Nippon Kagaku Kaishi* **1973**, 1119. (b) Wieghardt, K.; Bossek, U.; Guttmann, M.; Weiss, J. *Z. Naturforsch., B: Anorg. Chem., Org. Chem.* **1983**, *38B*, 81. (c) Sayer, B. A.; Michael, J. P.; Hancock, R. D. *Inorg. Chim. Acta* **1983**, *77*, L63. (d) Gahan, L. R.; Lawrence, G. A.; Sargeson, A. M. *Aust. J. Chem.* **1982**, *35*, 1119. (e) Polikarpov, M. Yu.; Shcherbakov, B. K.; Bel'skii, F. I.; Medved, T. Ya.; Kabachnik, M. I. *Izv. Akad. Nauk SSSR, Ser. Khim.* **1982**, 1669. (f) Christiansen, L.; Hendrickson, D. N.; Toftlund, H.; Wilson, S. R.; Xie, C. L. *Inorg. Chem.* **1986**, *25*, 2813. (g) Wieghardt, K.; Schöffmann, E.; Nuber, B.; Weiss, J. *Inorg. Chem.* **1986**, *25*, 4877. (h) DiVaira, M.; Mani, F.; Stoppioni, P. *J. Chem. Soc., Chem. Commun.* **1989**, 126.
(4) Moore, D. A.; Fanwick, P. E.; Welch, M. J. *Inorg. Chem.* **1989**, *28*, 1504.
(5) Richman, J. E.; Atkins, T. J. *J. Am. Chem. Soc.* **1974**, *96*, 2268.
(6) (a) Range, R. *Tetrahedron* **1971**, *27*, 1499. (b) Karlin, K. D.; Cohen, B. I.; Hayes, J. C.; Farooq, A.; Zubieta, J. *Inorg. Chem.* **1987**, *26*, 147.

0020-1669/90/1329-0938$02.50/0 